Temperature, carbon dioxide and methane

Clive Hambler (clive.hambler@zoo.ox.ac.uk)
University of Oxford
Peter A. Henderson
University of Oxford

Research Article

Keywords: Climate change, Degassing, Fractionation, Isotope, Outgassing, Productivity, Proxy

Posted Date: January 12th, 2022

DOI: https://doi.org/10.21203/rs.3.rs-558940/v2

Temperature, carbon dioxide and methane

Clive Hambler (1)*, Peter A. Henderson (1,2)

(1) Department of Zoology, University of Oxford, UK, ORCID 0000-0002-2361-828X (2) PISCES Conservation Ltd, UK, ORCID 0000-0002-7461-1758 * corresponding author clive.hambler@zoo.ox.ac.uk

Abstract

1) Globally-representative monthly rates of change of atmospheric carbon dioxide and methane are compared with global rates of change of sea ice and with Arctic and Antarctic air temperatures. 2) Carbon dioxide is very strongly correlated with sea ice dynamics, with the carbon dioxide rate at Mauna Loa lagging sea ice extent rate by 7 months. 3) Methane is very strongly correlated with sea ice dynamics, with the global (and Mauna Loa) methane rate lagging sea ice extent rate by 5 months. 4) Sea ice melt rate peaks in very tight synchrony with temperature in each Hemisphere. 5) The very high synchrony of the two gases is most parsimoniously explained by a common causality acting in both Hemispheres. 6) Time lags between variables indicate primary drivers of the gas dynamics are due to solar action on the polar regions, not mid-latitudes as is conventionally believed. 7) Results are consistent with a proposed role of a high-latitude temperature-dependent abiotic variable such as sea ice in the annual cycles of carbon dioxide and methane. 8) If sea ice does not drive the net flux of these gases, it is a highly precise proxy for whatever does. 9) Potential mechanisms should be investigated urgently.

Keywords Climate change • Degassing • Fractionation • Isotope • Outgassing • Productivity • Proxy

Introduction

The atmospheric levels of carbon dioxide have risen during the instrumental record (IPCC 2013). Superimposed on the trend are seasonal cycles. At Mauna Loa, Hawaii, carbon dioxide cycles are very regular and levels typically peak in May of each year, whilst methane, which is less regular, peaks around November. The amplitude of these cycles is generally highest in northern high latitudes, with some recording sites being exceptions and methane variation being more complex in the Northern Hemisphere (Fung et al 1991; Dlugokencky et al 1994; He et al 2017, Dlugokencky et al 2020; Saunois et al 2020; Hambler & Henderson 2020a, b).

The seasonal cycle of carbon dioxide is typically ascribed to the cycles of terrestrial productivity on the large land masses of the Northern Hemisphere, generating high seasonal amplitude at Arctic sites such as Barrow and Alert and with low amplitude at the South Pole and other Antarctic sites (Heimann et al 1989; Keeling et al 1989; Keeling et al 2001, 2005; Buermann et al 2007; Keeling 2008; IPCC 2013; He et al 2017; Jiang & Yung 2019). Similarly, the seasonal cycle of methane is typically ascribed to the cycle of wetland and agricultural and livestock production (with large sources on the land masses of the Northern Hemisphere) and to destruction by the OH radical in summer months in each Hemisphere (Fung et al 1991; Dlugokencky et al 1994).

However, the seasonal cycles of carbon dioxide and methane are both very strongly correlated with the seasonal cycle of sea ice, suggesting sea ice could have a dominant causal role in the cycle or is extremely strongly correlated with whatever does (Nelson & Nelson 2016; Hambler & Henderson 2020a, b). This unexpected observation requires explanation and invites the hypothesis that high-latitude temperature drives the dynamics of these gases. Temperature drives ice melt and should thus be very highly correlated with the monthly rate of change of these greenhouse gasses - whether or not sea ice is involved in the cycles. We test this prediction here.

Temperature is conventionally believed to drive the annual cycles of methane and carbon dioxide through changes in vegetation and microbial productivity, including agriculture (IPCC 2013). Yet despite great efforts, there is substantial uncertainty in the locations and magnitudes of sources and sinks for these gases (Kort et al 2012; Zhao et al 2016; Resplandy et al 2018; Weber et al 2019; Winkler et al 2019; Green et al 2020; Copernicus 2019; Saunois et al 2020; Harris et al 2021) with polar regions and areas of melting sea ice being amongst the most poorly known

due to challenging logistics (Vancoppenolle & Tedesco 2017; Geilfus et al 2018; Bushinsky et al 2019; MOSAiC 2019).

The locations of sources and sinks of carbon dioxide have traditionally been estimated using 'inversions' and 'atmospheric transport' models which rely on climate models to reverse-engineer from observed gas levels where major fluxes occur (*e.g.* Keeling et al 1989; Hein et al 1997; Beer et al 2010; Sitch et al 2015; Zhao et al 2016; Saunois et al 2020). Similarly, for methane, inversions and machine learning models have predicted where and when major ocean-atmosphere fluxes occur (such as shallow and Arctic and biologically productive waters) using sparse samples (Dlugokencky et al 1994; Weber et al 2019; Saunois et al 2020). We suggest an improvement on this method is to look at the similarity and synchrony of observed monthly rates of change of the gases with observations of potential causal variables, locally and globally. A dominant causal variable should be most strongly correlated with the global rate - with least temporal lag between timeseries of the gas rate and its local driver and with co-varying annual amplitudes. Of course, any seasonal variables such as livestock activity or wetland productivity or sea ice extent will have correlations with methane and carbon dioxide seasonality, but the spatial pattern of lags between timeseries can help identify the more likely causes and locations. For example, a polar causal variable should have a relatively high correlation and low lag with a positive gas flux near the pole.

Terrestrial productivity in the Northern Hemisphere is typically measured by NDVI (Keeling et al 1989; Keeling et al 2001; Buermann et al 2007) which is less strongly correlated with carbon dioxide rates than are sea ice rates (Hambler & Henderson 2020a); to our knowledge no region has been shown to have extremely high temporal synchrony and hence statistical correlation with the global carbon dioxide rate. Buermann et al (2007) do not present correlations of $r > 0.7$, and include significance values of $p < 0.1$. A "strong" correlation coefficient of 0.74 between the seasonal cycle amplitude of carbon dioxide and Northern Hemisphere land NDVI was detected by He et al (2017), with the highest local correlations between carbon dioxide levels and NDVI discovered being $r > 0.9$. Oceanic fluxes have been deduced using a grid showing cohesion between temperature anomaly and carbon dioxide levels at Mauna Loa (Park 2009).

Given the relatively strong correlations we have found with sea ice (Hambler & Henderson 2020a, b), we predict very strong synchrony between polar air temperatures and the high latitude fluxes of methane and carbon dioxide

(driven mainly by the annual cycle of solar elevation). We hypothesize high-latitude air temperatures drive sea ice dynamics and snow dynamics and thence might influence greenhouse gas dynamics. Such strong relationships are not presented in the review of the carbon cycle that informs international climate policy (IPCC 2013) and could focus greater attention on high latitude sites and fluxes.

Stable isotope ratios in carbon dioxide have been used to attempt to explain the seasonal variation in carbon dioxide and the contribution of human emissions to the trend in carbon dioxide (Heimann et al 1989; Keeling et al 2005). The monthly $^{13}C/^{12}C$ ratio co-varies closely and inversely with carbon dioxide in many recording stations, typically attributed to plants selectively fixing ^{12}C in photosynthesis in the Northern Hemisphere land masses, leaving uncertainty on the driver of the seasonal cycle in the Southern Hemisphere (Keeling et al 2005). The low proportion of ^{13}C in the Northern Hemisphere is attributed to a northern dominance of anthropogenic emission of carbon dioxide from fossil fuel sources which contain high ^{12}C (Keeling et al 2005).

However, carbon isotopic fractionation can occur by other processes, including microbial digestion and kinetic fractionation of methane (Damm et al 2015) and kinetic fractionation during freezing, degassing and carbonate crystal formation which causes a lighter isotopic composition in expelled carbon dioxide whilst ^{13}C is preferentially included in precipitated carbonate (Niles et al 2007). We therefore examine the relationship between sea ice melt and freeze rates and the proportion of the heavy isotope in the atmosphere ($\delta^{13}C$).

Methods

We use the datasets in Table 1.

Variable	**Data source**
Atmospheric CO_2 Mauna Loa, Alert and South Pole Monthly flask	NOAA GML Carbon Cycle Cooperative Global Air Sampling Network, 1983-2019, Version: 2020-07-24 https://www.esrl.noaa.gov/gmd/dv/data/ ftp://aftp.cmdl.noaa.gov/data/trace_gases/co2/flask Accessed 1 August 2020 Dlugokencky et al (2020a)

(Table 1 continued) Atmospheric CH_4 Mauna Loa, Alert, Cape Grim and South Pole Monthly flask	NOAA GML Carbon Cycle Cooperative Global Air Sampling Network, 1983-2019, Version: 2020-07-24 https://www.esrl.noaa.gov/gmd/dv/data/ ftp://aftp.cmdl.noaa.gov/data/trace_gases/ch4/flask Accessed 1 August 2020 Dlugokencky et al (2020b)
Atmospheric CH_4 Globally-averaged monthly data	https://esrl.noaa.gov/gmd/ccgg/trends_ch4/ Accessed 1 January 2021 Dlugokencky (2021)
Atmospheric stable isotope C13 in CO_2 $\delta^{13}C = [(13C/12Csample/(^{13}C/^{12}Cstandard/)-1] \times 1000$ Monthly flask	https://www.esrl.noaa.gov/gmd/dv/data/ Accessed 27 December 2021 White et al (2015)
Atmospheric methyl chloroform Gas chromatograph hourly samples	Methyl chloroform data from the NOAA/ESRL halocarbons in situ program https://www.esrl.noaa.gov/gmd/dv/data/ Accessed 29 March 2021
NDVI	MDOIS satellite imagery MOD13C2 product as 5 kilometre monthly mean global imagery Accessed July 2019
Sea ice extent Monthly mean	https://nsidc.org/data/seaice_index/archives Sea Ice Index Version 3 ftp://sidads.colorado.edu/DATASETS/NOAA/G02135/ (Fetterer et al 2017) 'North' (= 'Arctic'): ftp://sidads.colorado.edu//DATASETS/NOAA/G02135/north/monthly/data/ at sidads.colorado.edu 'South' (= 'Antarctic'): ftp://sidads.colorado.edu/DATASETS/NOAA/G02135/south/monthly/data/ Files in form: S_01_extent_v3.0.csv Accessed 26 February 2020 ftp://sidads.colorado.edu/DATASETS/NOAA/G02186/ MASIE NSIDC/NIC Sea Ice Product G02186 - Daily Ice Extent by Region in Square Kilometers National Ice Center and National Snow and Ice Data Center. Compiled by F. Fetterer, M. Savoie, S. Helfrich, and P. Clemente-Colón. 2010, updated daily. Multisensor Analyzed Sea Ice Extent - Northern Hemisphere (MASIE-NH),

(Table 1 continued)	Version 1. Subset: 4km. Boulder, Colorado USA. NSIDC: National Snow and Ice Data Center. doi: https://doi.org/10.7265/N5GT5K3K Accessed 5 February 2020
Sea ice volume, Arctic Modelled by DMI Monthly mean	http://ocean.dmi.dk/arctic/index.uk.php http://ocean.dmi.dk/arctic/icethickness/txt/IceVol.txt Accessed 23 July 2019
Snow extent Northern Hemisphere Monthly mean	https://climate.rutgers.edu/snowcover/docs.php?target=datareq NH SCE CDR v01r01 https://climate.rutgers.edu/snowcover/files/moncov.namgnld.txt https://climate.rutgers.edu/snowcover/files/moncov.nam.txt Accessed 27 March 2020
Alert air temperature Monthly mean	NCEP Reanalysis Dataset Produced at NOAA Physical Sciences laboratory https://psl.noaa.gov/data/timeseries/arctic/ Accessed 6 January 2021
South Pole air temperature (Amundsen-Scott South Pole Station) Monthly mean	Amundsen_Scott temperature https://legacy.bas.ac.uk/met/READER/surface/Amundsen_Scott.All.temperature.txt British Antarctic Survey. UK Antarctic Surface Meteorology; 1947 - 2013 http://dx.doi.org/10.5285/569d53fb-9b90-47a6-b3ca-26306e696706 Accessed 16 December 2020

Table 1 Data sources

We examine atmospheric gas levels for a site considered globally representative for carbon dioxide (Mauna Loa, Hawaii, USA) (IPCC 2013), and a global average estimate of monthly methane (Dlugokencky 2021). We also examine methane rates at Mauna Loa since these are measurements from what might also be a representative site for methane.

Within the NOAA Global Monitoring Laboratory network of atmospheric gas recording sites we examine the most northerly site (Alert, Canada) and the most southerly (South Pole) since these would be predicted to respond strongly to any temperature-dependent forcing. Having examined all sites in this network with monthly flask data we selected Cape Grim (Tasmania, Australia, latitude 41°S) as an illustration of the high similarity of phenology of the South Pole to some sites at lower latitudes.

We do not use models of atmospheric transport of gas but instead make the minimalistic assumption that gas from a polar region will take longer to reach or cross the equator than to reach nearby sites. We assume the shape of the seasonal gas flux curve will be most similar to the curve of the causal variable near the site of the causal variable (due to mixing).

Temperature data (average monthly values in degrees Centigrade) were obtained for meteorological stations at the South Pole and Alert as examples of very high-latitude sites where local gas levels are also monitored. The Alert data were rescaled by subtracting 100, to make all values negative. Temperature values were inverted to visually compare synchrony of peak temperature with peak negative net fluxes of the gases, since we have previously established peak negative flux is tightly synchronous with sea ice melt at high latitudes (Hambler & Henderson 2020a, b).

Recording of the OH radical in the atmosphere is very difficult, so is usually done indirectly using methyl chloroform (CH_3CCl_3) which OH reacts with and hence lowers the atmospheric concentration (Ravishankara & Albritton 1995; Hein et al 1997; Reidel & Lassey 2008). In the annual cycle, low levels of methyl chloroform should correspond to high levels of OH.

We follow the classic use of NDVI to locate likely carbon dioxide fluxes due to terrestrial vegetation productivity (Keeling et al 1989; Buermann et al 2007; He et al 2017). There is high synchrony in monthly NDVI rates between the Northern Hemisphere latitudinal belts and continents (Hambler and Henderson 2020a) and thus for simplicity of presentation we selected data for North America and Eurasia, 35^{o}N to 70^{o}N, which has high amplitude (as does recorded carbon dioxide flux at northern high latitudes) and which captures a substantial area of these continents. Use of NDVI for the full Northern Hemisphere or a narrower high latitude belt would not affect our conclusions (Hambler & Henderson 2020a). We invert monthly data for NDVI to give an approximate measure of a lack of productivity (indicating periods which have a net carbon dioxide sink). These are rescaled by a factor of 1000 for clarity.

Methodological consistency is essential in time series analysis (Henderson 2021) so we use datasets which are very likely to have been quality controlled for methodological drift. A monthly database of sea ice extent is easily available from NSIDC from January 2006, which we therefore use as the start date. Arctic and Antarctic extents were used to calculate the rate for the 'global' sea ice extent (which we term 'Arctic plus Antarctic' rate as in Hambler & Henderson 2020a, b). Longer timeseries are available and presented for selected variables, such as the full continuous carbon dioxide record at Mauna Loa from July 1976, to visually assess if more recent years have a very different pattern.

Rates of change for variables were derived as follows: rate in month 2 is the mean value in month 2 minus the mean value in month 1.

Statistical analysis was based on the R platform. Cross correlations and consideration of autocorrelation were performed as in Hambler & Henderson (2020b). For pairs of time series, cross correlations and 95% confidence bounds for lags of up to +/- 12 months were calculated using the ccf function in the tseries R package. These results were used to identify the lag producing the highest correlation and the rcorr function then used to calculate the Pearson correlation and associated probability that it could be generated by random chance. Because we find probabilities are near zero for numerous of our results, which would require many digits to present, significance values are all presented as $p < 0.001$.

Due to data availability and other constraints at the time of this work, some time series have different end dates or missing values so are not fully comparable and not all are analysed statistically. Statistical analyses are only performed here for the global levels of methane and carbon dioxide and for one other time series for illustrative purposes (showing a tight visual fit is also supported statistically). The results of any analysis are given in the Figure captions. Previous work (Hambler & Henderson 2020a, b and unpublished) has established that close visual fits using the minima in such time series always have high statistical correlations and often identify the lag between them; this can be confirmed if the work is replicated.

Results

a) Globally representative atmospheric gas measurements

The monthly time series for carbon dioxide rate from Mauna Loa, global sea ice extent rate and an Arctic temperature (Alert, Canada) are given in Fig. 1 and Fig. 2.

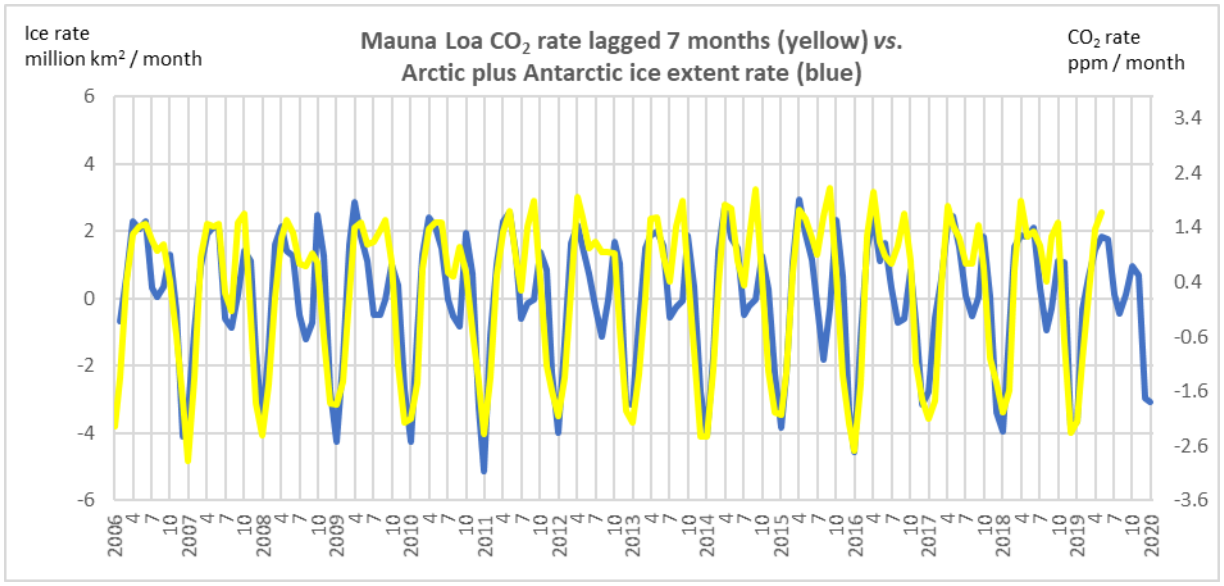

Fig. 1 Global monthly carbon dioxide rate (measured at Mauna Loa, lagged 7 months) *vs.* global sea ice extent rate. $r = 0.79$ at lag = 7 months; $p < 0.001$

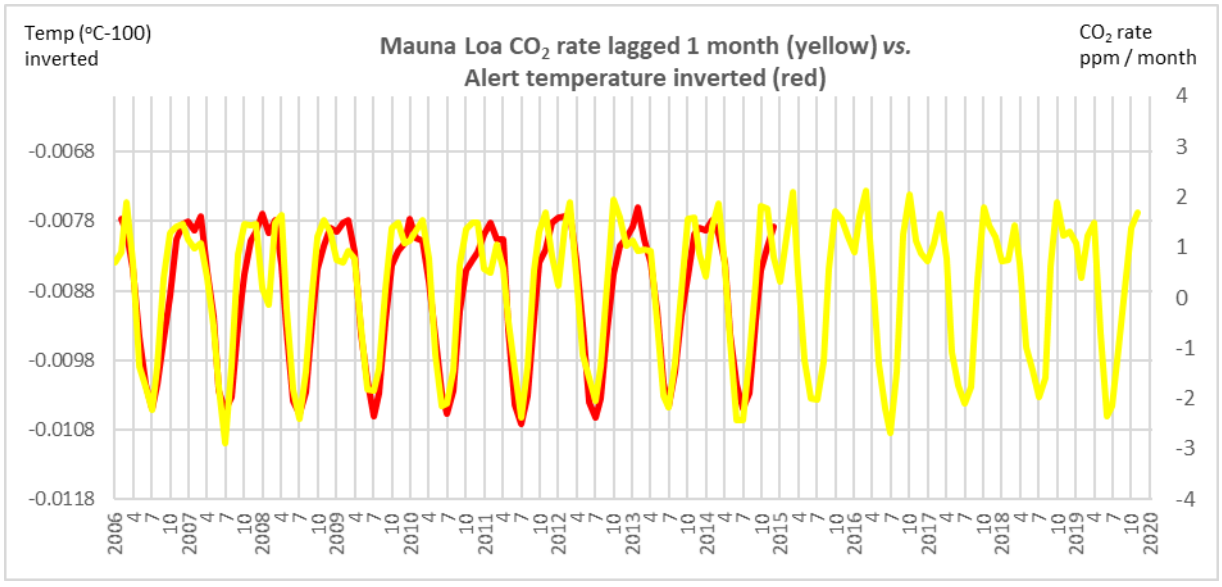

Fig. 2a Monthly carbon dioxide rate Mauna Loa (lagged 1 month) *vs.* temperature at Alert (inverted)

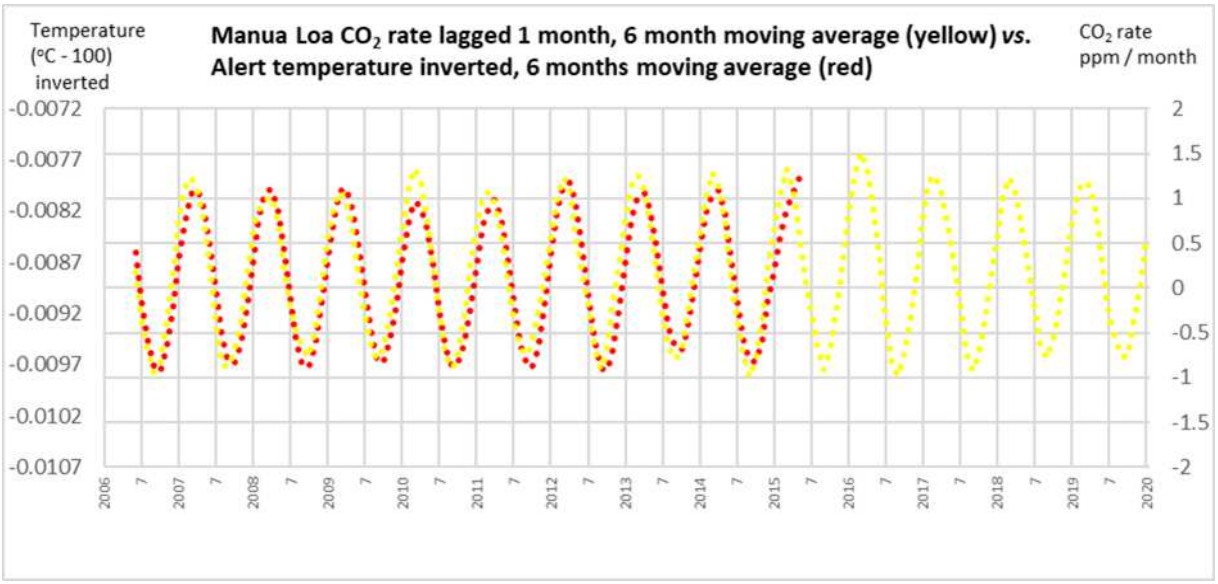

Fig. 2b Monthly carbon dioxide rate Mauna Loa (lagged 1 months) *vs*. temperature at Alert, Canada (inverted), 6 month moving average for both variables

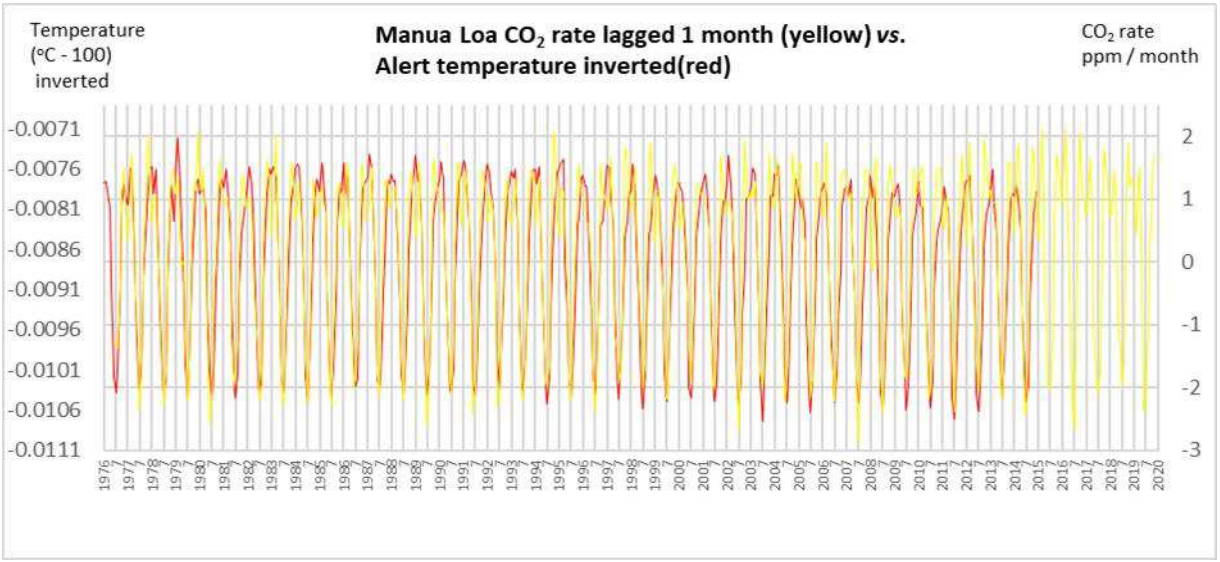

Fig. 2c Monthly carbon dioxide rate Mauna Loa (lagged 1 month) *vs*. temperature at Alert, Canada (inverted), using full continuous monthly Mauna Loa CO_2 record from July 1976

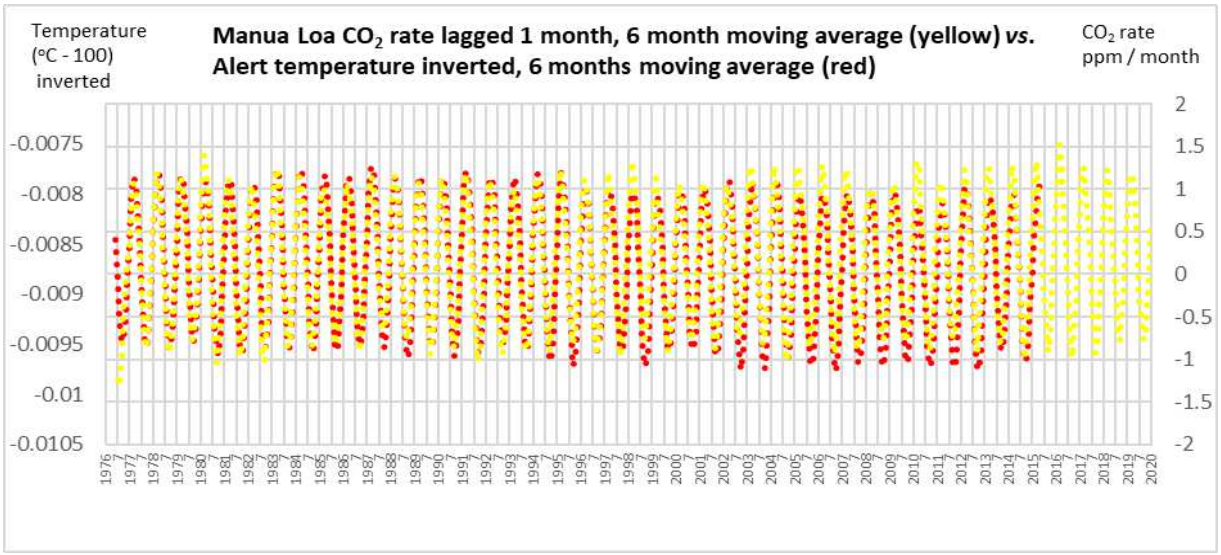

Fig. 2d Monthly carbon dioxide rate Mauna Loa (lagged 1 month) *vs.* temperature at Alert, Canada (inverted), 6 month moving average for both variables, using full continuous monthly Mauna Loa CO2 record from July 1976

The monthly time series for carbon dioxide rate from Mauna Loa and an Antarctic temperature (South Pole) are given in Fig. 3.

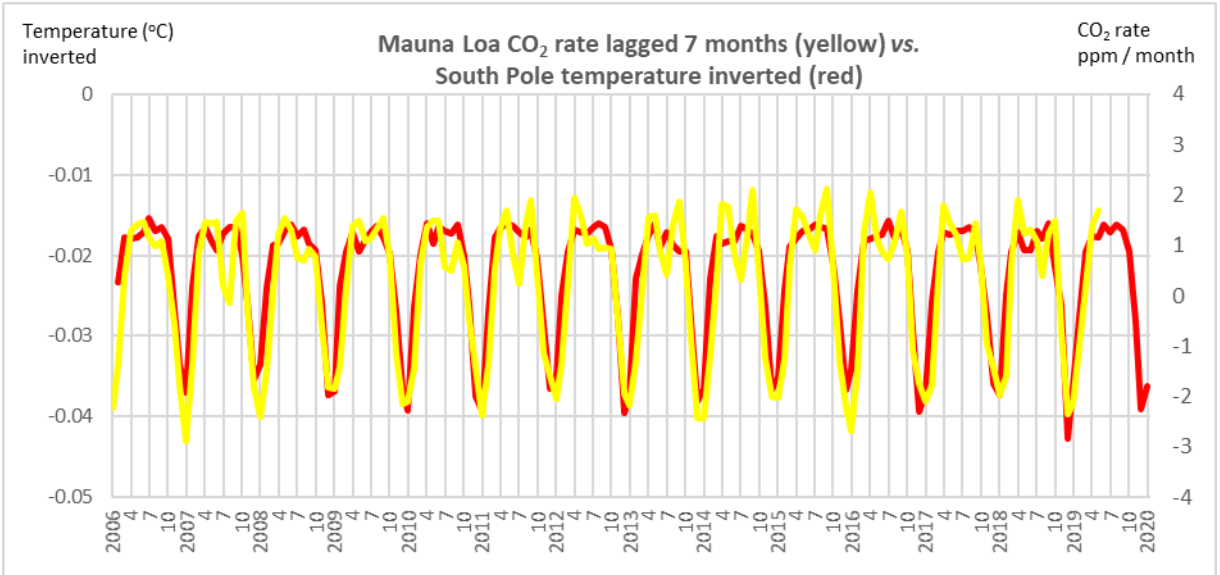

Fig. 3a Monthly carbon dioxide rate Mauna Loa (lagged 7 months) *vs.* temperature at South Pole (inverted)

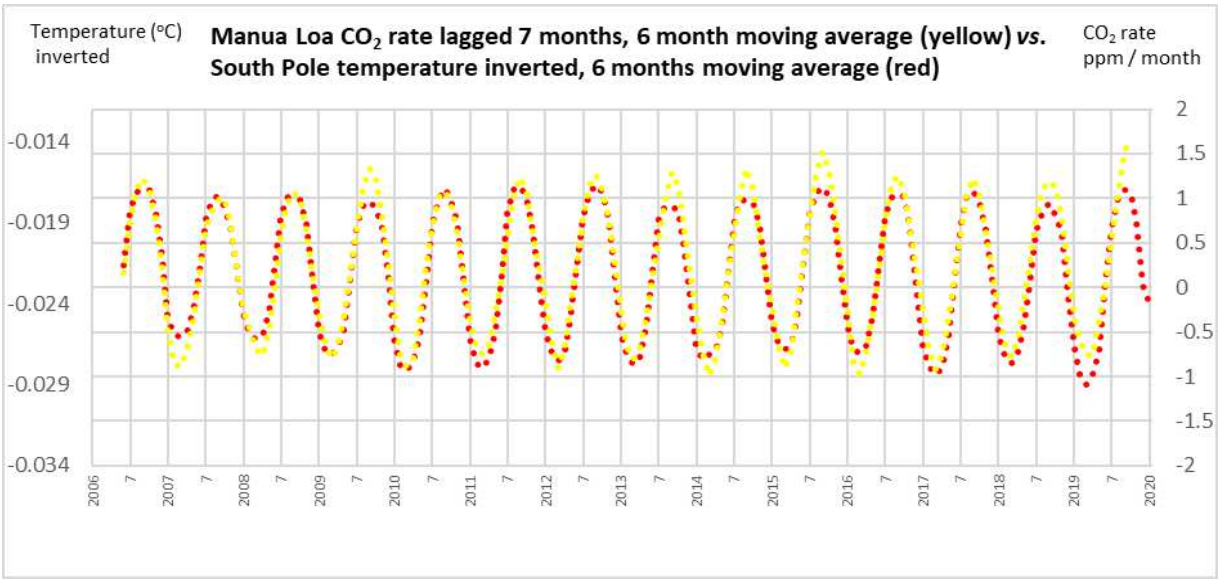

Fig. 3b Monthly carbon dioxide rate Mauna Loa (lagged 7 months) *vs*. temperature at South Pole (inverted), 6 month moving average for both variables

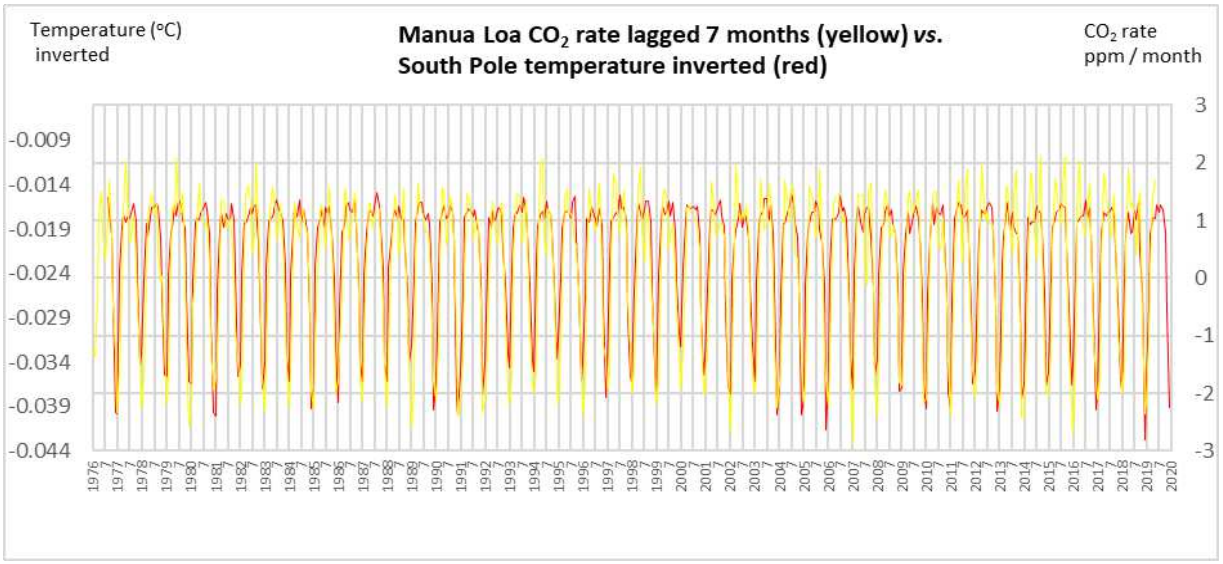

Fig. 3c Monthly carbon dioxide rate Mauna Loa (lagged 7 months) *vs.* temperature at South Pole (inverted), using full continuous monthly Mauna Loa CO_2 record from July 1976

The monthly time series for methane rates averaged from a global network of sites, and from Mauna Loa, are plotted against global sea ice extent rate in Fig. 4 and Fig. 5.

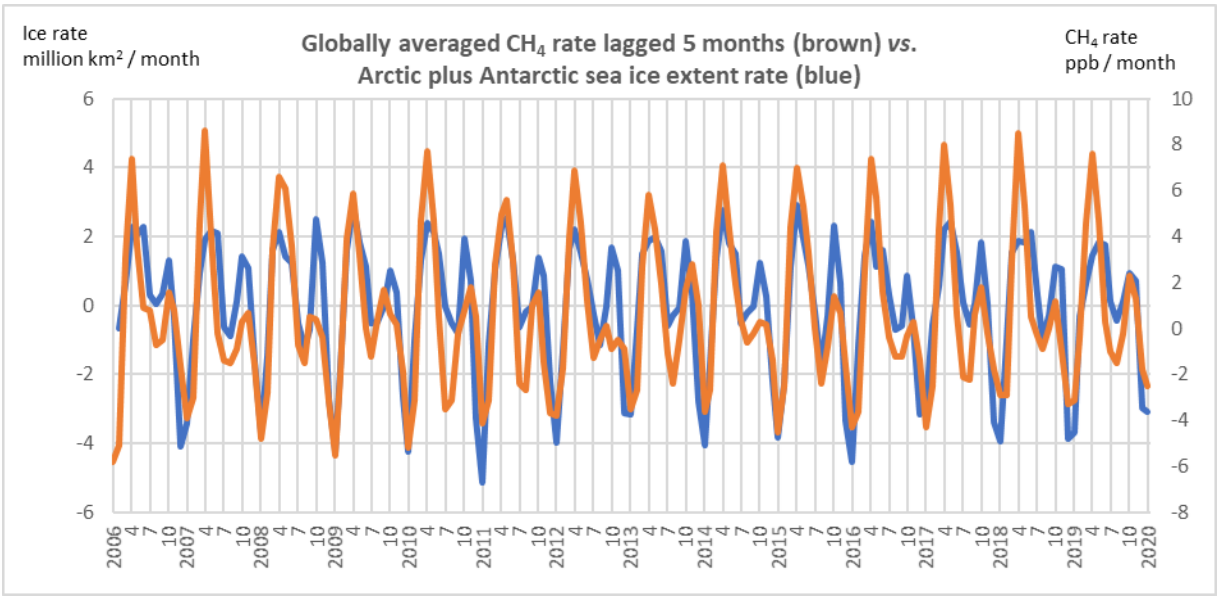

Fig. 4 Monthly global average methane rate (lagged 5 months) *vs.* global sea ice extent rate. $r = 0.78$ at lag = 5 months; $p < 0.001$

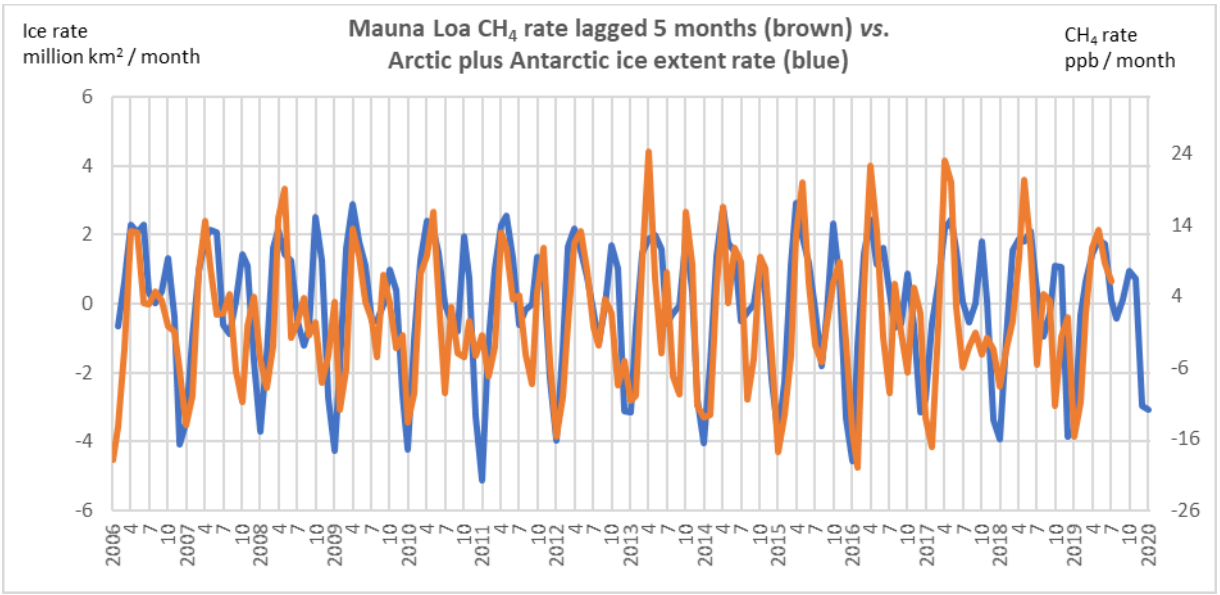

Fig. 5 Monthly methane rate Mauna Loa (lagged 5 months) *vs.* global sea ice extent rate

Globally representative carbon dioxide and methane rates are compared in Fig. 6.

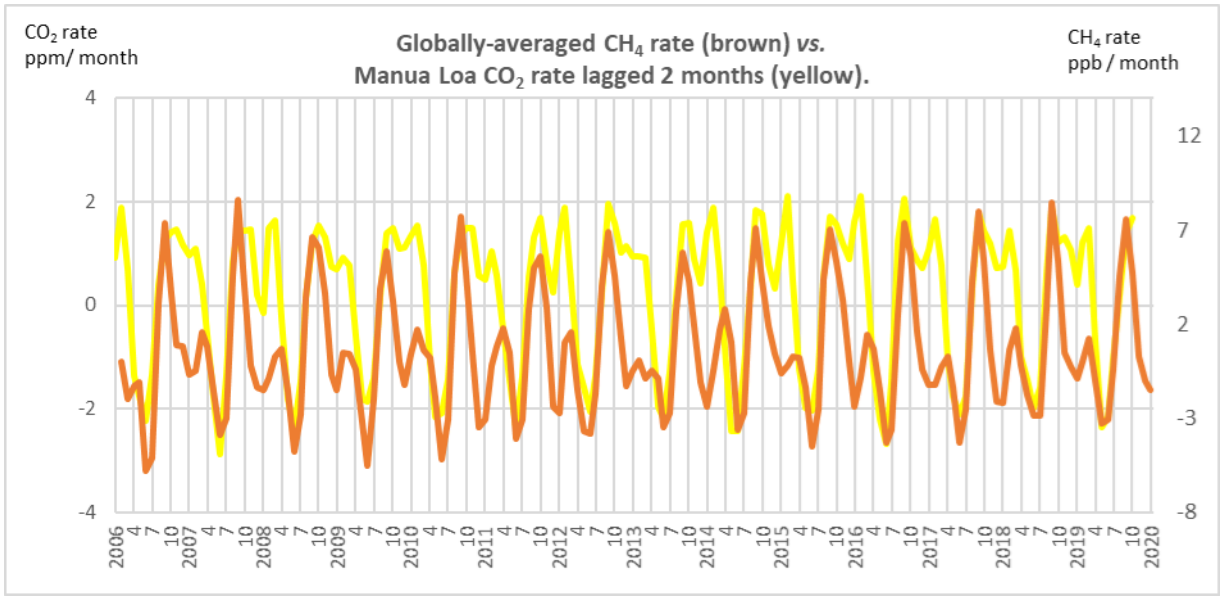

Fig. 6 Global carbon dioxide rate (Mauna Loa, lagged 2 months) *vs.* global methane rate

b) Arctic. Monthly time series for carbon dioxide and methane rates at Alert (Canada) plotted against Alert temperature and Northern Hemisphere snow extent rate, are given in Figs. 7 - 9.

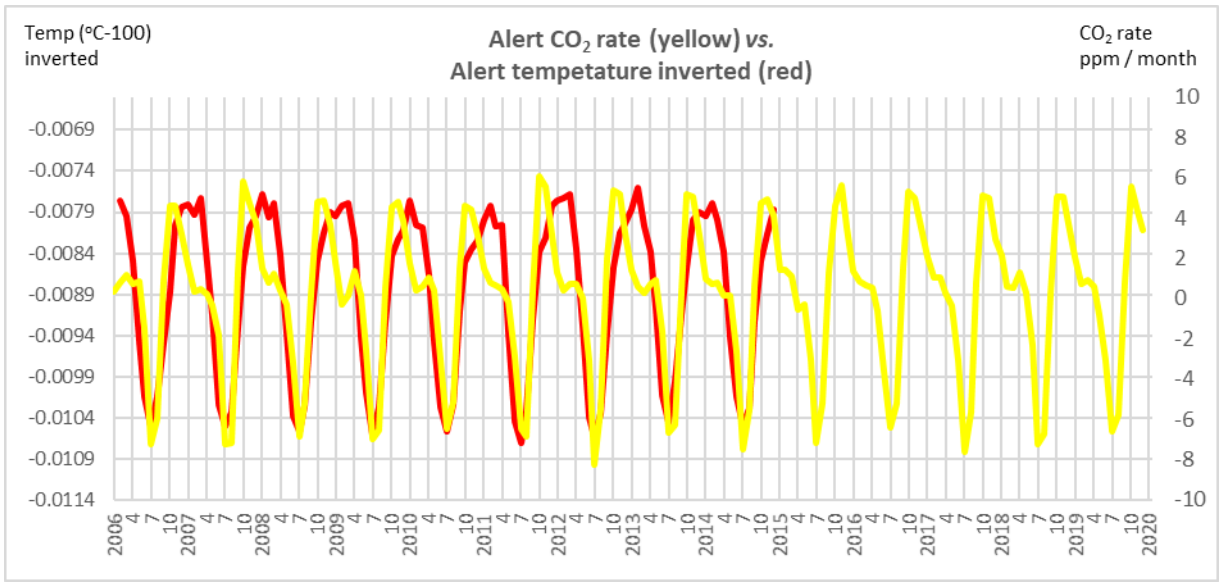

Fig. 7 Monthly carbon dioxide rate Alert *vs.* temperature at Alert (inverted)

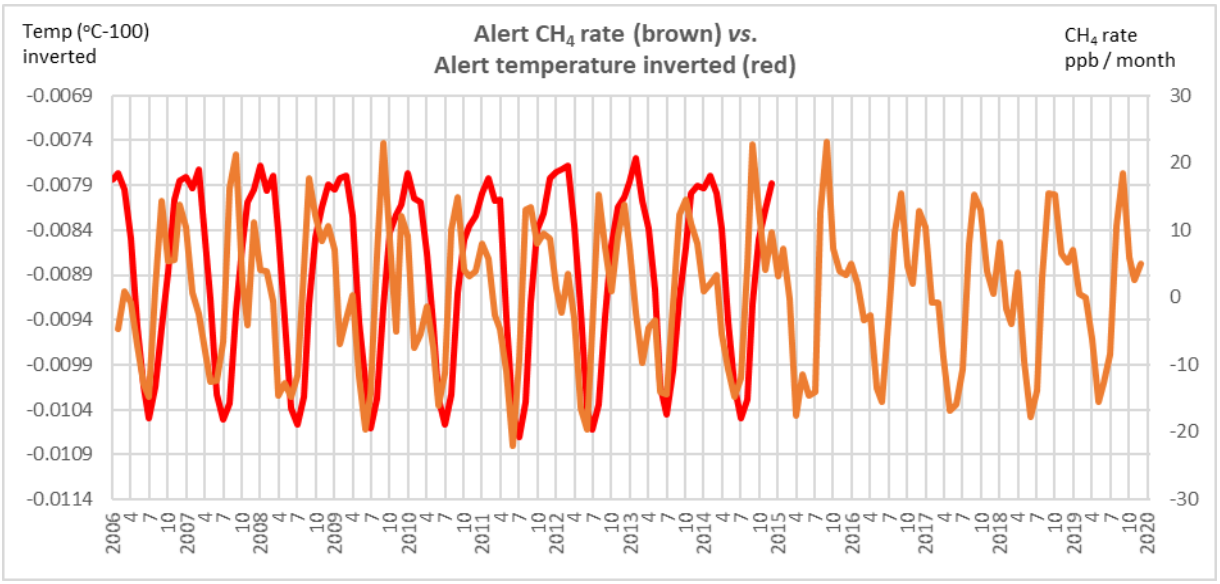

Fig. 8 Monthly methane rate Alert *vs.* temperature at Alert (inverted)

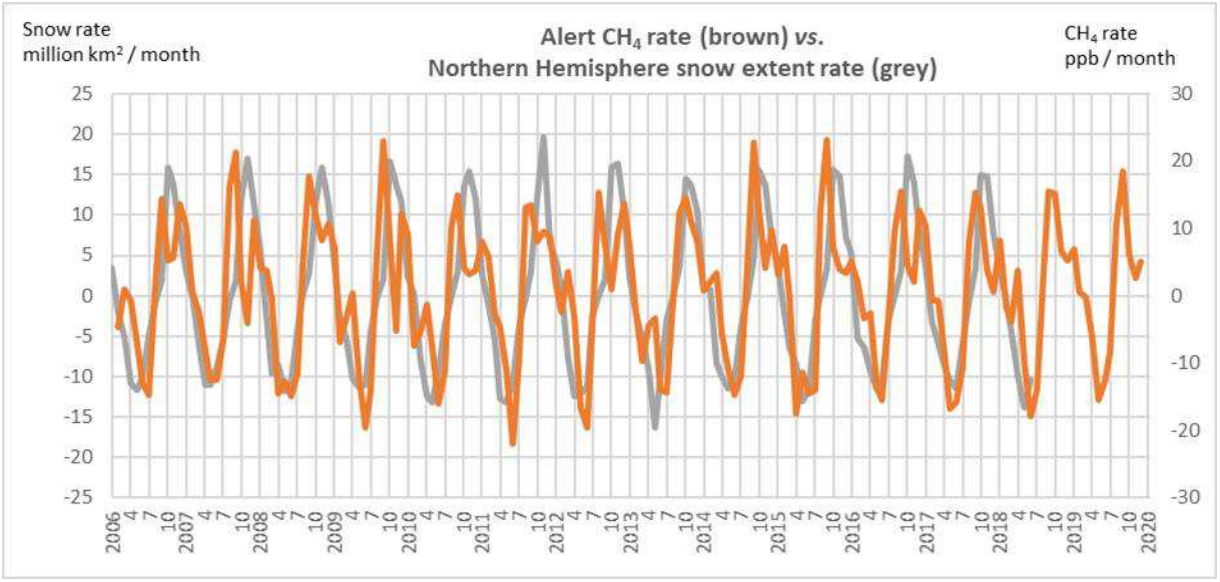

Fig. 9 Monthly methane rate Alert *vs.* Northern Hemisphere snow extent rate

Time series for Arctic sea ice extent rate and a local temperature (Alert) are given in Fig. 10.

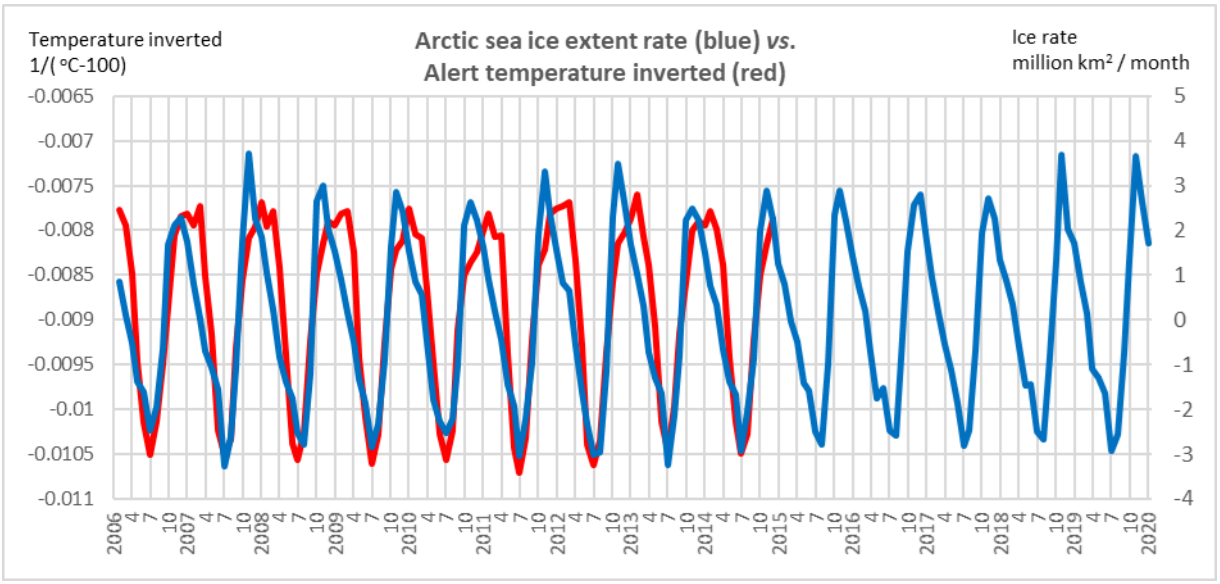

Fig. 10 Monthly Arctic sea ice extent rate *vs.* temperature at Alert (inverted)

c) Antarctic

Monthly time series of carbon dioxide rate and methane rate at the South Pole, and temperature at the South Pole, are given in Figs. 11 - 13.

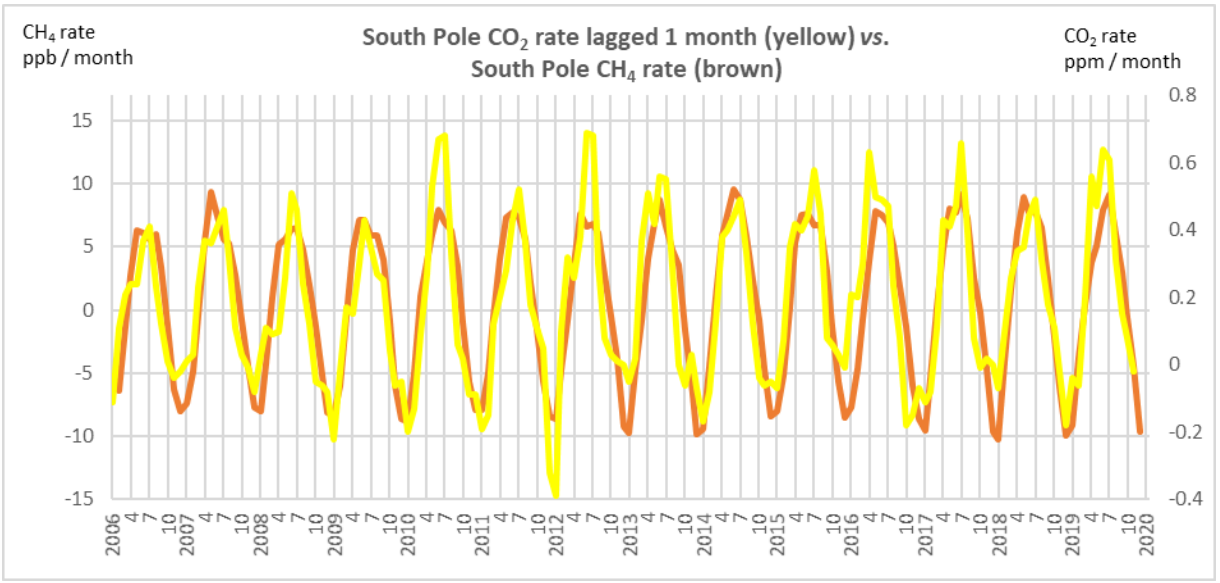

Fig. 11 Monthly carbon dioxide rate South Pole (lagged 1 month) *vs.* monthly methane rate South Pole

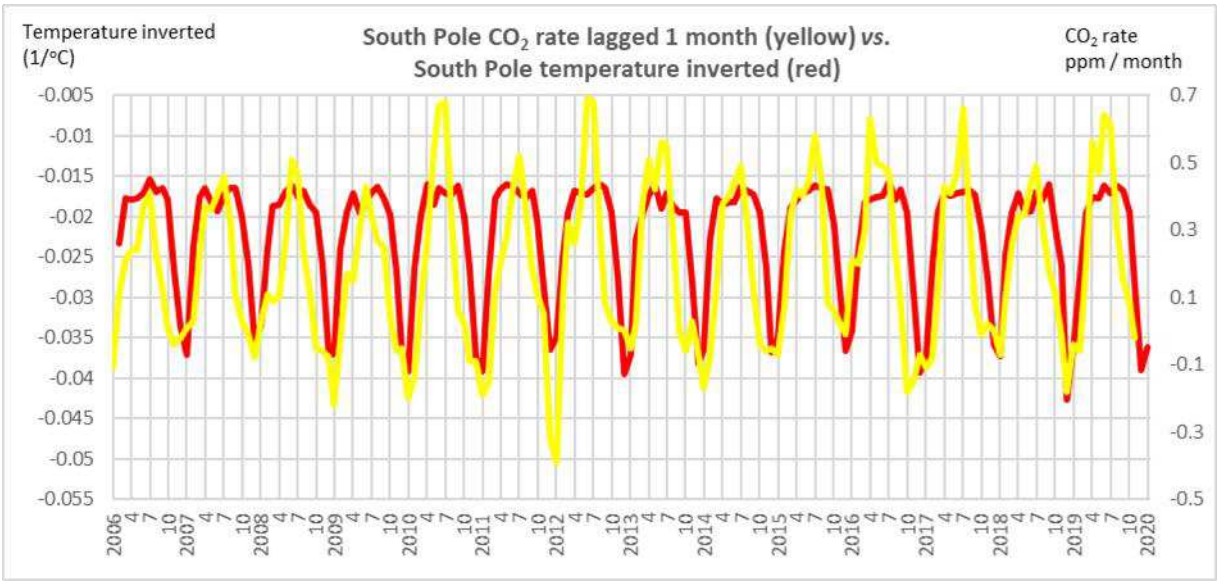

Fig. 12 Monthly carbon dioxide rate South Pole (lagged 1 month) *vs.* temperature at South Pole (inverted)

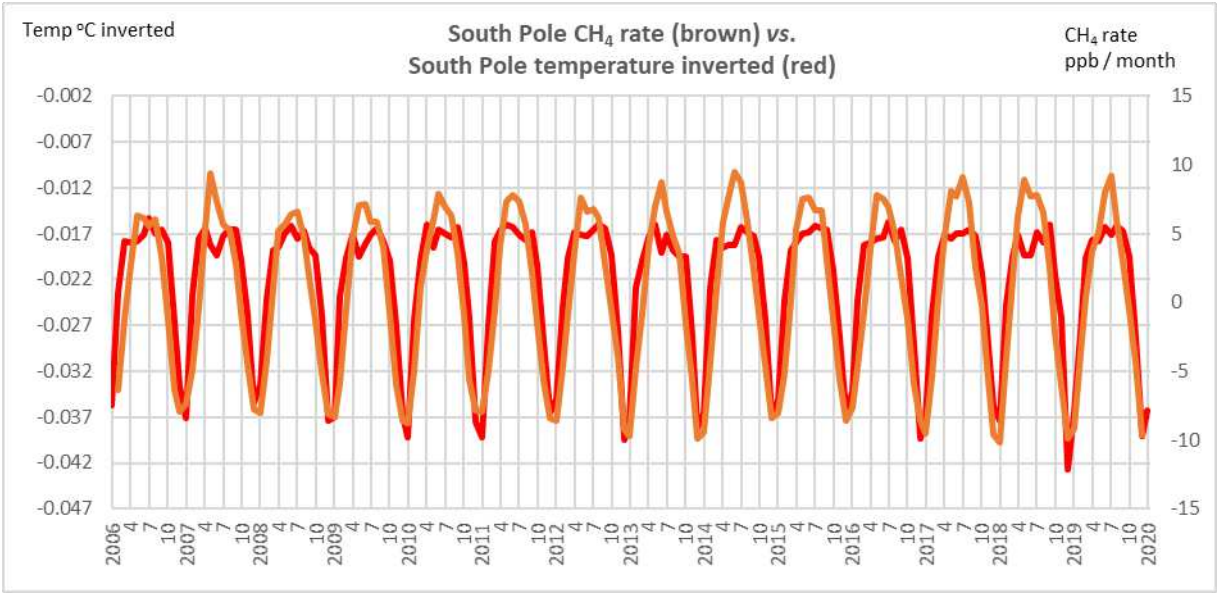

Fig. 13a Monthly methane rate South Pole *vs.* temperature at South Pole (inverted). $r = 0.88$ at zero lag; $p < 0.001$

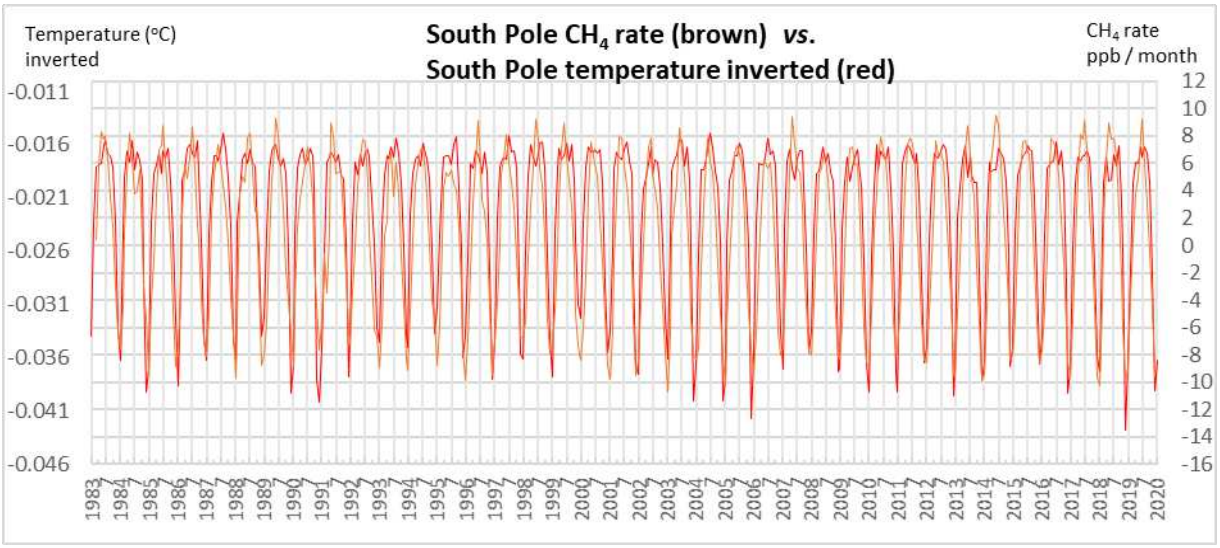

Fig. 13b Monthly South Pole methane rate *vs.* temperature at South Pole (inverted), using full continuous monthly methane record from February 1983

An example of the similarity of South Pole methane rate phenology to another Southern Hemisphere site, Cape Grim, is given in Fig. 14.

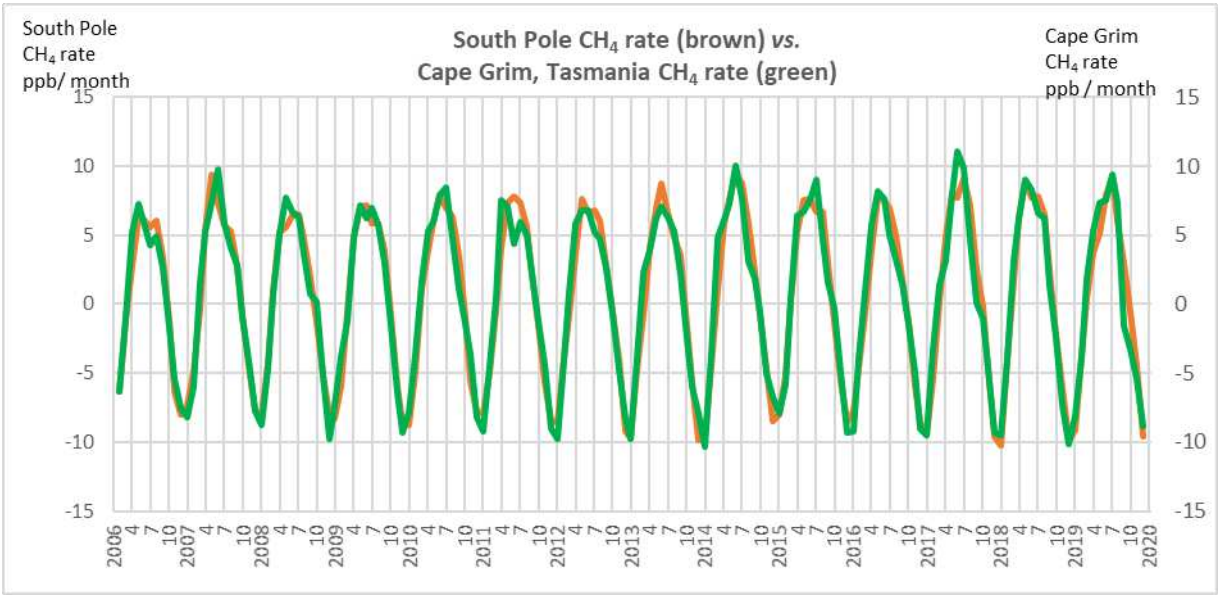

Fig. 14 Monthly methane rate South Pole *vs.* monthly methane rate Cape Grim (Tasmania)

Time series for Antarctic sea ice rate, a local temperature and South Pole methane rate are given in Figs. 15 and 16.

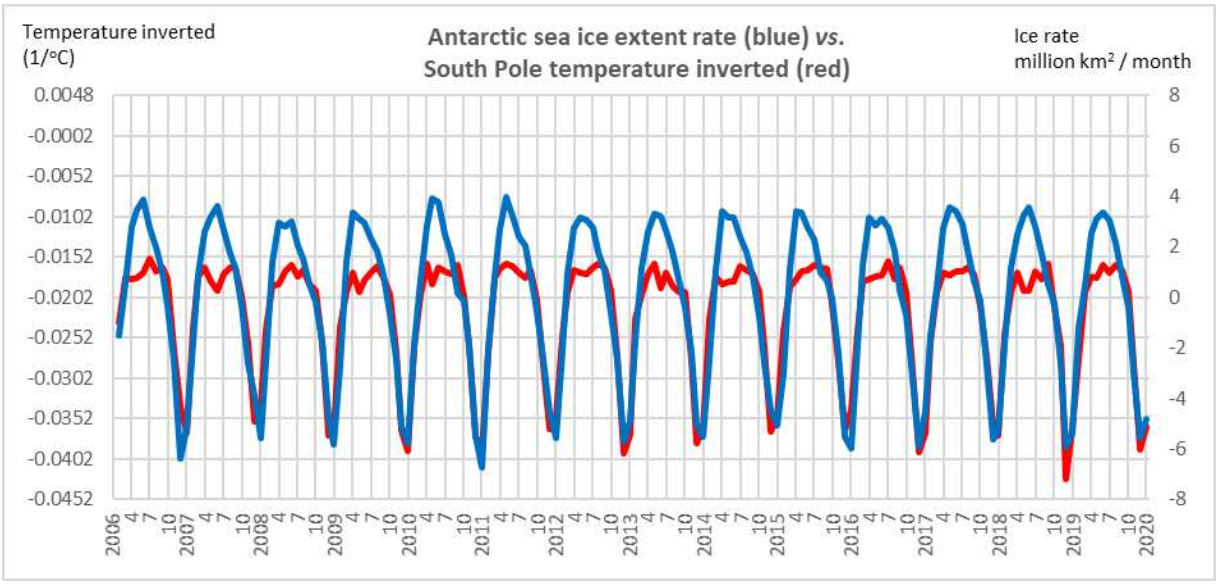

Fig. 15 Monthly Antarctic sea ice extent rate *vs.* temperature at South Pole (inverted)

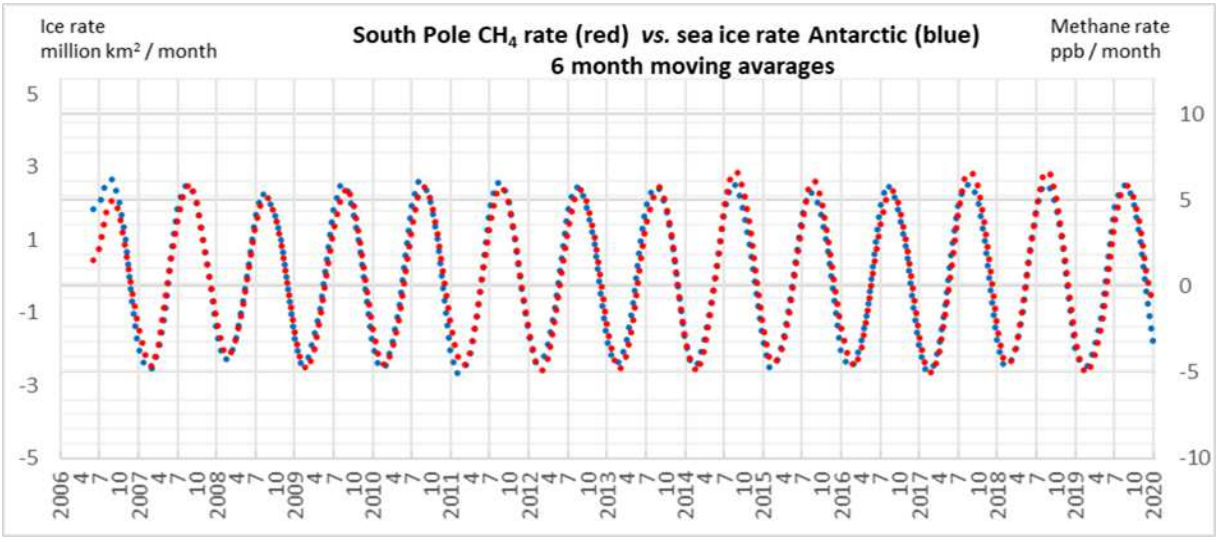

Fig. 16 Monthly Antarctic sea ice extent rate *vs.* monthly methane rate South Pole, 6 month moving average for both variables

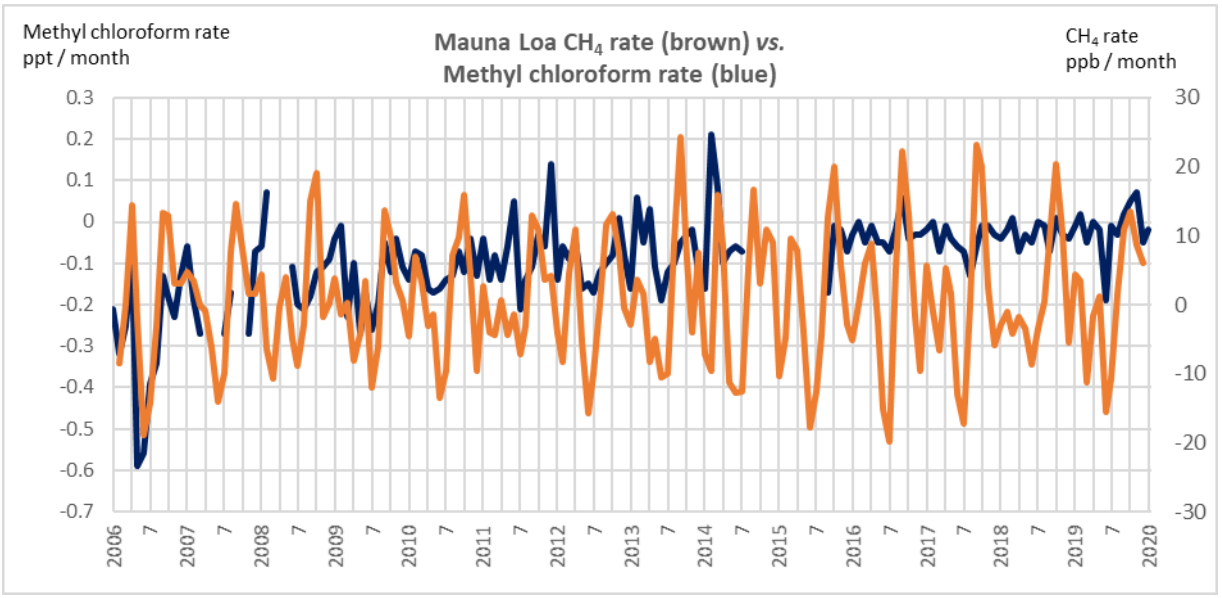

Fig. 17a Monthly methane rate Mauna Loa *vs.* monthly methyl chloroform rate Mauna Loa

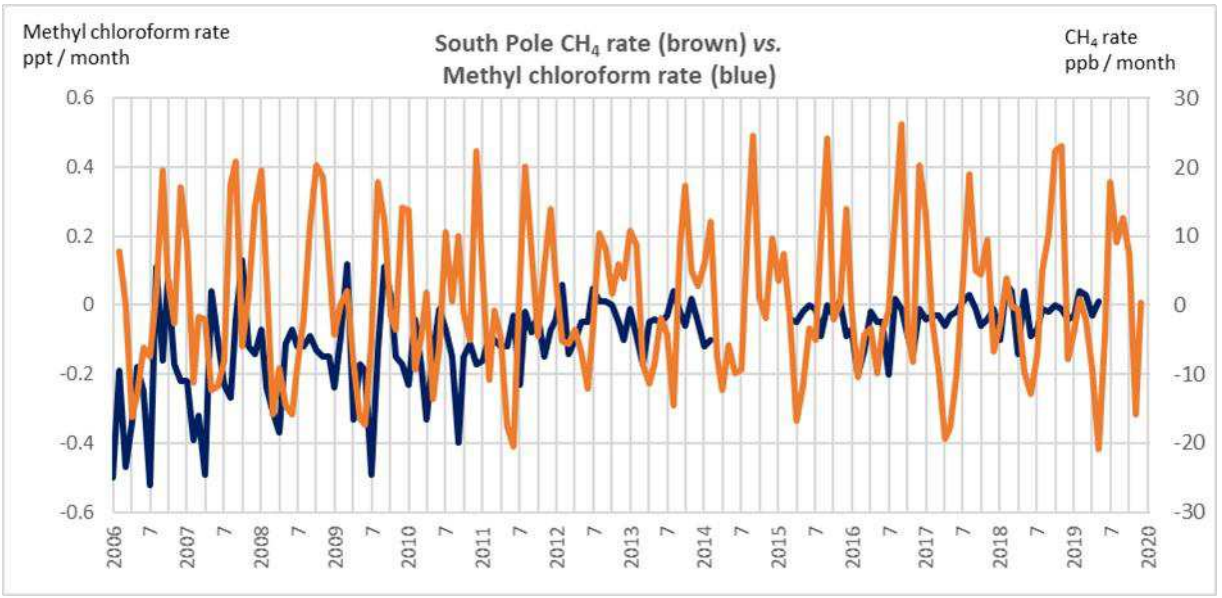

Fig. 17b Monthly methane rate South Pole *vs.* monthly methyl chloroform rate South Pole

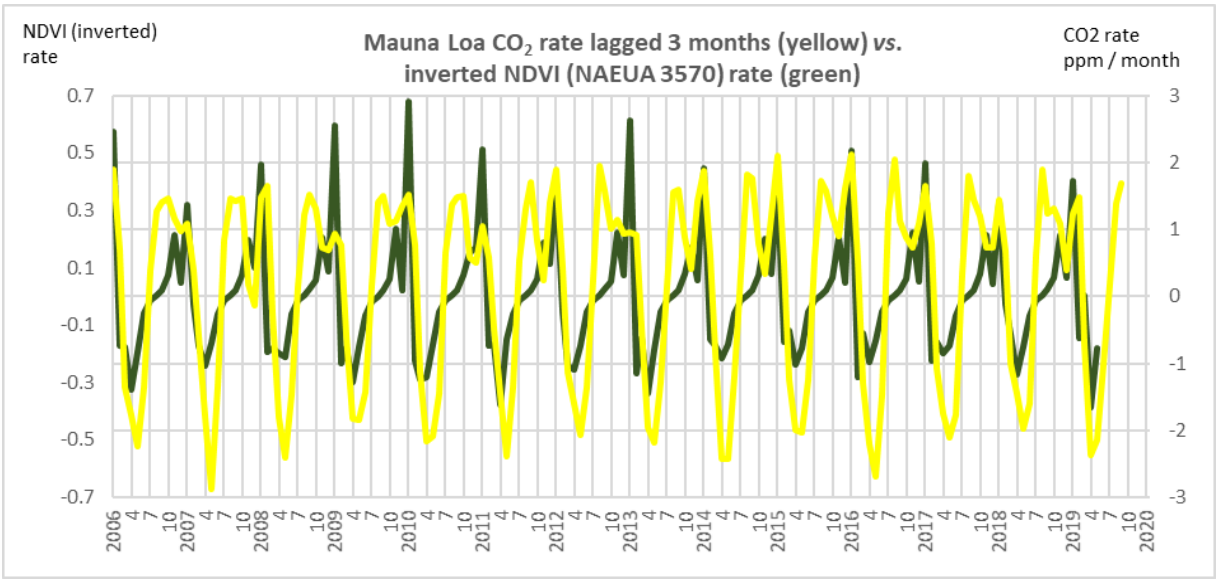

Fig. 18a Monthly carbon dioxide rate Mauna Loa (20ºN) lagged 3 months *vs*. monthly inverted NDVI rate North America and Eurasia, 35ºN to 70ºN (NAEUA3570)

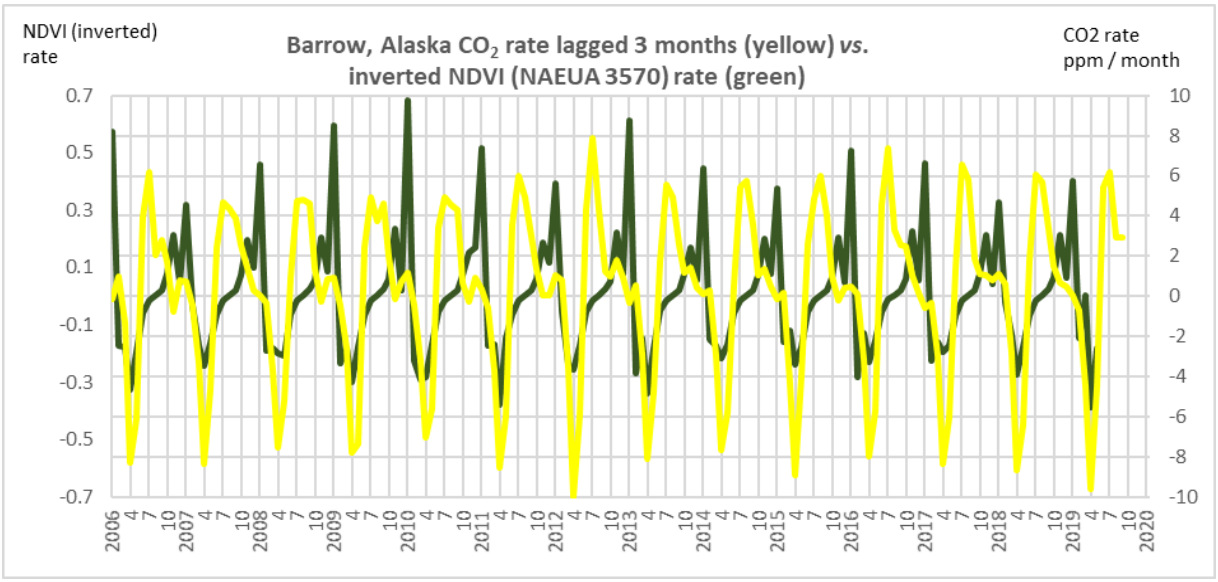

Fig. 18b Monthly carbon dioxide rate Barrow, Alaska (71ºN) lagged 3 months *vs*. monthly inverted NDVI rate North America and Eurasia, 35ºN to 70ºN (NAEUA3570)

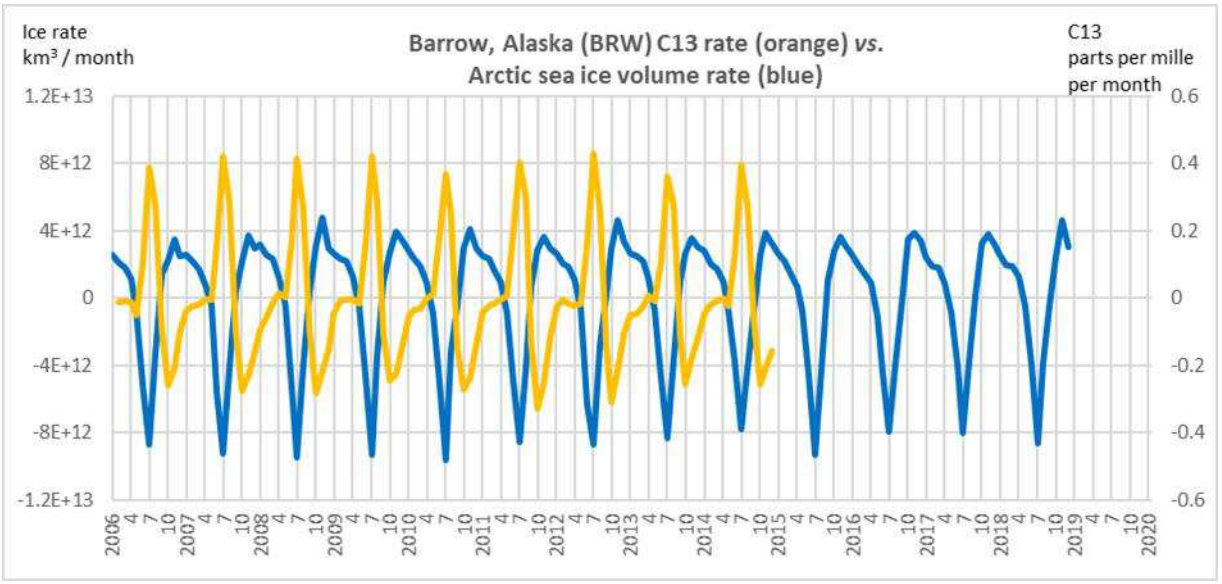

277
278 **Fig. 19** Monthly $\delta^{13}C$ rate Barrow, Alaska (71°N) *vs.* Arctic sea ice volume rate

279

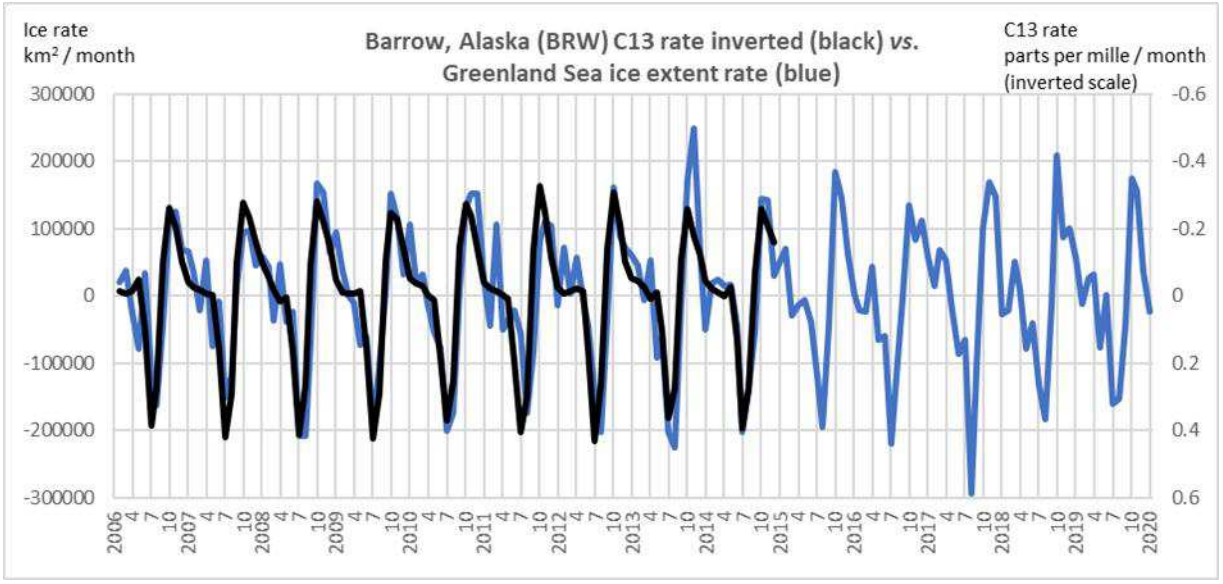

280
281 **Fig. 20** Monthly $\delta^{13}C$ rate Barrow, Alaska (inverted scale) *vs.* Greenland Sea sea ice extent rate

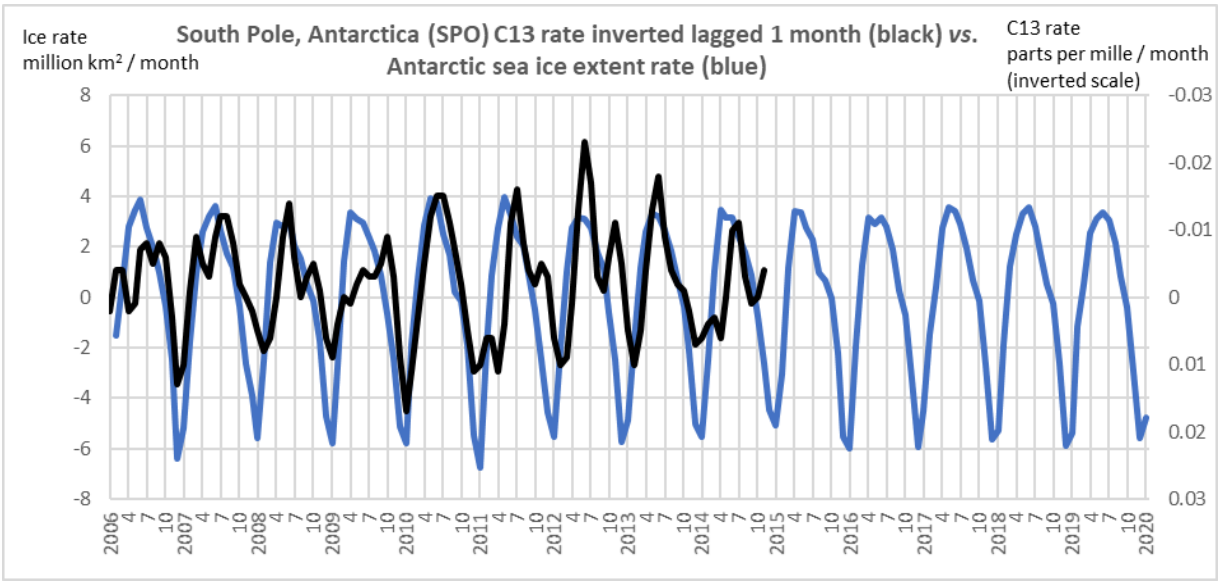

Fig. 21 Monthly $\delta^{13}C$ rate South Pole (inverted scale, lagged one month) *vs*. Antarctic sea ice extent rate

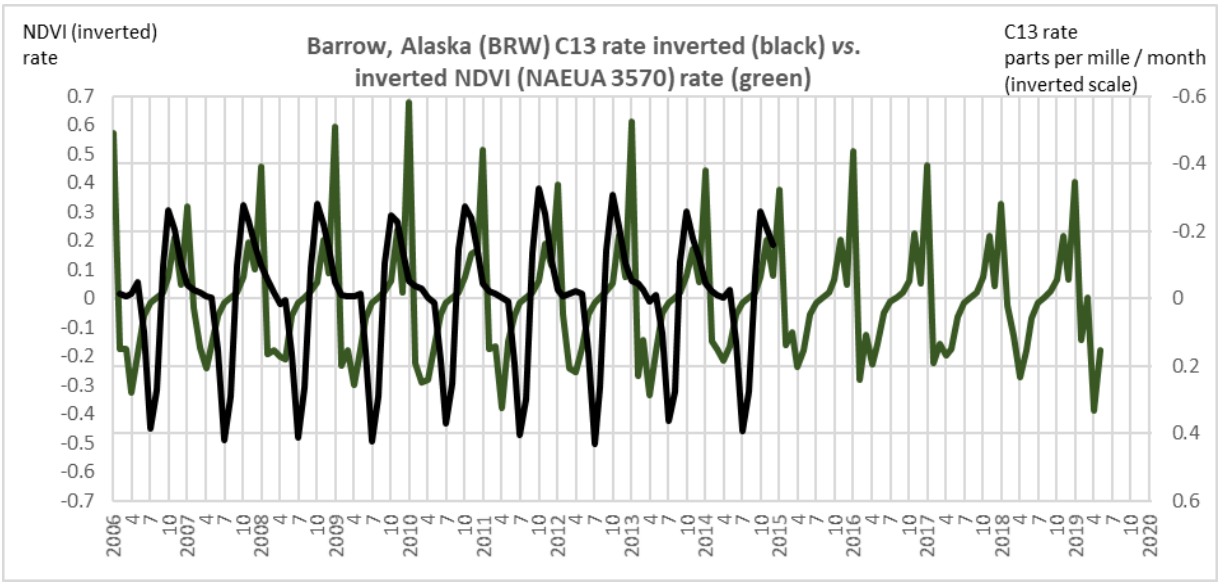

Fig. 22 Monthly $\delta^{13}C$ rate Barrow, Alaska (71ºN) (inverted scale) *vs*. monthly inverted NDVI rate North America and Eurasia, 35ºN to 70ºN (NAEUA3570).

Discussion

Air temperature at or near the Poles peaks in very close synchrony with regional peaks in sea ice melt (Figs. 10 and 15). It will also be correlated with a range of other abiotic and biotic variables with various lags, such as Northern Hemisphere snow (Fig. 9) and Greenland terrestrial ice melt. Air temperature at high latitude sites leads the global

carbon dioxide rate with a greater lag of carbon dioxide behind the Antarctic than the Arctic temperature (Fig. 2 and Fig. 3).

The rates of change of globally representative levels of carbon dioxide and methane are very strongly correlated with the rate of change of global ('Arctic plus Antarctic') sea ice (Figs. 1 and 4) on the timescales examined. The rate of change of methane at Mauna Loa has similar phenology but greater amplitude (Fig. 5). At the South Pole, methane rates are very highly synchronous with Antarctic sea ice extent rates (Fig. 16), as are other regional methane rates (Hambler & Henderson 2020b). The lag of 5 - 7 months between the peak Antarctic temperature (and sea ice melt) and the fastest decline of global methane and global carbon dioxide suggest a strong Antarctic influence on these gases (Fig. 1 and Fig. 4). It may take months for the effects of temperature on gas flux in the Antarctic to reach the Northern Hemisphere.

The extremely strong predictive power of global total sea ice for carbon dioxide and methane is notable - revealing possible causality or high predictive power for the actual cause. The two peaks in global sea ice rate result from the peak temperatures in the two Hemispheres. Global carbon dioxide and methane rates also have twin peaks which are similarly separated (Fig. 6). We propose that whatever dominates the fluxes of these gases makes strong contributions at high latitudes in both Hemispheres. For carbon dioxide we propose (on the basis of seasonal amplitudes and lags) that there is a particularly strong contribution from sea ice melt and calcium carbonate dissolution in the Greenland area (Hambler & Henderson 2020a).

Temperature in at least one Arctic recording site has a close synchrony with carbon dioxide (Fig. 7) and methane (Fig. 8) flux rates at the site (Alert, Canada). Other high-latitude Northern Hemisphere recording sites in the NOAA network have similar carbon dioxide and methane phenology to Alert (Hambler & Henderson, 2020a, b). Peak negative carbon dioxide flux (indicating drawdown or destruction of the gas) usually occurs synchronously with peak atmospheric temperature in the Arctic summer (July, Fig. 7). This is also synchronous with peak decline in Arctic ice extent (Fig. 10). However, peak negative methane flux at Alert (Fig. 8) occurs about one month earlier than peak temperature and peak sea ice melt in the whole Arctic, which we suggest results from an influence of the biota or other abiotic factors on methane dynamics in the Arctic. Arctic sea ice as a whole can not be the dominant causal variable in this region at least, but there are regional differences in sea ice phenology, and Alert methane peak

decline is more closely synchronous with the Barents Sea ice rate (Hambler & Henderson, unpublished). Peak rate of decline of Arctic methane is also closely synchronous with peak snow extent decline in the Northern Hemisphere, with Alert lagging snow melt rate by about a month (Fig. 9), consistent with putative terrestrial influences such as increased methanogenic microbial activity. Peak methane emission from Arctic mires can occur near peak summer air temperature (Jackowicz-Korczyński et al 2010).

Peak negative methane flux at the South Pole is synchronous with peak temperature at the South Pole (Fig. 13) but carbon dioxide rate at the South Pole lags one month behind the peak temperature which occurs December / January (Fig. 12). Similarly, methane rates slightly lead carbon dioxide rates globally and at Mauna Loa (Figs. 4 - 6). Intriguingly, South Pole temperature peaks simultaneously with peak rates of decline in both methane and carbon dioxide at the coastal and marine Antarctic sites in the NOAA network (Palmer, Syowa, Halley, Drake Passage) and is also simultaneous with peak Antarctic sea ice melt (Hambler & Henderson, 2020a, b). There may be differential transport, production or removal processes for methane and carbon dioxide after a synchronous monthly pattern is imprinted in the two gases at the edge of the Antarctic continent. High latitude sites in the Southern Hemisphere have very similar methane phenology (*e.g*. Fig. 14 and Hambler & Henderson 2020b) suggesting a very well-mixed southern air mass (as per Dlugokencky et al 1994) and / or a large-scale causal process.

The synchronous decline and rise in carbon dioxide and methane at many sites would most parsimoniously be explained by a single mechanism. These results are broadly consistent with our proposals that sea ice is either involved in the decline of atmospheric carbon dioxide and methane or is extremely strongly corelated with an unknown variable causing fluxes of the gases (Hambler & Henderson 2020a, b). We argue the extremely high correlations between sea ice and fluxes of both gases are more plausibly due to simple physical or chemical processes than to ecological ones (Hambler & Henderson 2020a, b). In particular, we suggest the peak negative gas rates may relate to ice melt and absorption by cold water undersaturated in these gases (Wiesenburg & Guinasso Jr 1979). Similarly, ocean temperature was suggested to drive lagged carbon dioxide changes through solubility changes (Park 2009). The peak positive rates may relate to expulsion of gas during sea ice formation (degassing), marine emissions during summer warming of the ocean and from upwelling, and other physical and biological processes (Vancoppenolle et al 2013; Vancoppenolle & Tedesco 2017; Hambler & Henderson 2020a, b). Mechanisms coupling sea ice and the atmosphere (such as brine drainage, modulation of upwelling, and ikaite

dissolution cycles) are not yet well represented qualitatively or quantitatively in biogeochemical models (Kort et al 2012; Vancoppenolle et al 2013; Damm et al 2015; Vancoppenolle & Tedesco 2017) and their magnitudes may have been underestimated.

High latitude oceans and sea ice are amongst the few places currently recorded as having frequent net emission of CO_2. Studies with emission and / or absorption phenologies we find broadly consistent with our hypothesis include: Ishii et al (2002); Semiletov et al (2007); Bakker et al (2008); Nomura et al (2010, 2013, 2014, 2018); Sejr et al (2011); Fransson et al (2011, 2017); Shadwick et al (2011); Vancoppenolle et al (2013); Geilfus et al (2013, 2014, 2015, 2018); Roden (2016); Brown et al (2015); Butterworth & Miller (2016); Prytherch et al (2017); Tison et al (2017); Vancoppenolle & Tedesco (2017); Gray et al (2018); Søgaard et al (2019); Ouyang et al (2020). This selection of studies is not systematic but provides examples of fluxes and of the types of research that will be necessary to test predictions on representative spatial and temporal scales.

The conventional explanation of the terrestrial biota of the Northern Hemisphere driving the carbon dioxide seasonal cycle (Keeling et al 1989; Keeling et al 2001, 2005; Buermann et al 2007; Keeling 2008; IPCC 2013; He et al 2017; Jiang & Yung 2019) does not explain the similar patterns of global carbon dioxide and methane which have many different biological and abiotic sources and sinks (IPCC 2013). The similar patterns of seasonal variation of CO_2 concentration and ^{13}C isotopic fraction at several locations is puzzling if the fractionation mechanism is biotic and predominantly northern (Keeling et al 2005) but not if it is physical and the same in both Hemispheres. Isotopes are in any case of limited use in identifying carbon fluxes because different sources can have the same fractions (Salby 2012).

Measured by NDVI, terrestrial productivity has relatively weak synchrony and curve shape similarity with carbon dioxide rates, in any large region, even with lags (Fig.18; Hambler & Henderson 2020a), making this a less likely driver than sea ice rates despite common belief. For the period 2003-2018 inclusive, the cross correlation between sea ice volume and carbon dioxide rates ($r = 0.90$) is stronger than between NDVI (35°N -70°N) and carbon dioxide rates ($r = 0.62$), Hambler & Henderson (2020a). Alternatively, NDVI may be of limited value in detecting carbon fixation rates (Welp et al 2016) despite its conventional use for this purpose - and dependence of flux on precipitation or other factors affecting productivity and respiration might be expected to introduce noise and weaken

the relationship further. Terrestrial fluxes of carbon dioxide are not as well known as many imagine, and much recent data has been surprising - as with periods of emission from tropical forests or large fluxes over deserts (*e.g.* Mearns 2015; Qin et al 2021). Those supporting the conventional 'consensus' view have yet to locate areas of the planet with such strong correlations as we find with global carbon dioxide rates - yet probably have an intuitive feeling such areas exist since this is easier to accept than to reject the current paradigm.

A major factor implicated in removing atmospheric methane, the hydroxyl radical (OH) (Dlugokencky et al 1994; Mastepanov et al 2008; Salby 2012; Ciais et al 2013) is created by photodissociation and thus would be expected to be temperature-dependent with latitudinal variation in amplitude. Indeed, OH concentration is highest in the tropics (Hein et al 1997; Reidel & Lassey 2008). If as is widely assumed OH is dominant in global methane dynamics it would be expected to cause lagged fluxes of methane at the polar sites. The seasonal low of methane *level* near the South Pole occurs when OH is assumed high in the austral summer (Dlugokencky et al 1994). However, methane rate lags further behind peak temperature nearer the equator (Hambler & Henderson 2020b) suggesting net methane loss is not fastest where there is most sunlight. The relationship between methane rates and methyl chloroform rates is relatively weak (*e.g.* Fig. 17 and Hambler & Henderson, unpublished). Moreover, to our knowledge there is no reported directly causal reason for OH to vary synchronously with carbon dioxide rate (as it often does regionally). Indeed, the positive modelled correlation between marine methane emission and photosynthetic productivity (Weber et al 2019) would argue against synchrony with carbon dioxide release.

A lag of 7 months between temperature and carbon dioxide rate is consistent with the observed lag of about 9 - 10 months between temperature and carbon dioxide level (Humlum et al 2013; Salby 2013), suggesting South Pole air temperature is a very good proxy for a variable driving the annual carbon cycle. South Pole air temperature and Antarctic sea ice extent rate should both have predictive power for the 'global' carbon dioxide level 10 months in advance. Our results are consistent with a proposed sequence of events driving carbon dioxide changes starting in the Southern Hemisphere (Humlum et al 2013). Tropical ocean temperature anomaly is also significantly coherent with lagged carbon dioxide level (Park 2009); temperature fluctuations at gridpoints in North East America and the North Atlantic but not polar regions were also significantly coherent with Mauna Loa carbon dioxide fluctuations; it is possible the difference from our result reflects Park's use of the Hadley Centre's HadCrut3 temperature anomaly, rather than temperature, and carbon dioxide levels, rather than rates.

Isotope ratio rate clearly co-varies closely with sea ice rate (Figs. 19 - 21) although these are not analysed statistically since the isotopic time series is available for only part of the timeframe that we consider for carbon dioxide and methane. During sea ice formation in either hemisphere the ratio of ^{13}C to ^{12}C declines in the atmosphere; this is consistent with degassing of carbon dioxide enriched in ^{12}C, as demonstrated experimentally (Niles et al 2015). Notably, the transition dates between positive and negative rates are near synchronous for $\delta^{13}C$ and Arctic sea ice volume (Fig. 19). The visual similarity between isotope rate and sea ice rate is closer for Barrow (Fig. 20) than for the South Pole (Fig. 21), and amplitudes are greater and more constant at Barrow. These features (and similar results for other polar sites, Hambler & Henderson unpublished) are consistent with fractionation being stronger in the Northern Hemisphere. At Barrow, there is an interesting close similarity of isotope rate to sea ice rate in the Greenland Sea (Fig. 20), as there is with carbon dioxide rate and Greenland Sea ice rate (Hambler & Henderson 2020a).

In contrast to these near-simultaneous changes of rate of sea ice and isotopes, the northern photosynthetic rate of change, approximated by NDVI rate, does not have a closely similar pattern to $\delta^{13}C$ rate (Fig. 22) with periods of fast $\delta^{13}C$ increase lagging fast increase photosynthetic activity by about 4 months. If examined with satellites and ground-truthed in the field, such a lag might present a discriminating test of the seasonal source of enriched ^{13}C in carbon dioxide. The phenology of terrestrial respiration and decay releasing ^{12}C requires further investigation since peak fractionation rate may not coincide precisely with peak NDVI rate or peak NDVI.

Critiques of our methods and conclusions might suggest that there are stronger terrestrial flux correlations with the gas rates that have yet to be identified, and that the recorded quantities (moles) of carbon dioxide or methane in sea ice are insufficient to cause the global flux changes. Our results are indeed inconsistent with current estimates of gas budgets (*e.g.* Dlugokencky et al 1994; Ciais et al 2013; Saunois et al 2020). Our response is that it is circular reasoning to use existing sampling of quantities and flux measurements to argue our predictions on under-sampled quantities must be wrong. Falsification of our hypotheses would require much more comprehensive spatial and temporal coverage of gas levels (such as satellites might provide). Whilst some carbon stores (such as in sea ice itself) might be lower than we predict, a combination of several temperature-dependent fluxes and stores in the carbon cycle might combine to reach the magnitudes required. Although sparse, many measurements of carbon

dioxide phenology in polar regions show similar timings of positive and negative fluxes that are in general agreement with an involvement of sea ice and calcium carbonate (ikaite) dissolution (Vancoppenolle et al 2013; Hambler & Henderson 2020a). However, high temporal and spatial variability suggests determination of net annual flux from all regions will require hourly, or daily, consistent sampling at large scales and more systematic analysis. Analyses and animations of the globe showing rates of change of gases, rather than levels, may be particularly informative and convincing; it is intriguing to see radiative forcing and / or carbon dioxide concentration peaking seasonally near the poles in a relatively spatially comprehensive analysis - which merits further serious investigation (Rentsch 2021a, b).

Inter-annual variation in monthly rates leads to net accumulation or loss of methane and carbon dioxide from the atmosphere. Both the amplitude and phase of methane rates in many sites in the Southern Hemisphere south of about 25°S are very similar (Hambler & Henderson 2020b, and *e.g.* Fig. 14) suggesting large-scale common forcing. A variable such as temperature which correlates strongly with the amplitude of the annual cycle (*e.g.* Fig. 13) could help explain net global trends: for example, warm years generally have higher sea ice melt rates and more negative gas rates which might be partially caused by dissolution in melt water and changes in upwelling of gas-laden water. The monthly timeseries of sea ice extent we use (Table 1) are presumably created with relatively consistent methods between years but are only provided since 2006. There may be too little statistical power to examine in detail relationships between sea ice and annual rate - but Hambler & Henderson (2020a) demonstrate annual carbon dioxide rates correlate strongly with global and oceanic lower tropospheric temperature and thus mechanisms involving ice could be hypothesized. The selected longer timeseries we have examined do not suggest recent years are anomalous (Fig. 2c; Fig. 2d; Fig. 3c; and Fig.13b) and these warrant further analysis.

Conclusions

We suggest other variables be examined that might be influenced by temperature or insolation which might drive fluxes of carbon dioxide and methane. These include, for example, marine and terrestrial productivity, upwelling rates, sea temperature depth profiles, glacial and ice shelf melt and calving, winds, and the hydroxyl radical (for methane). Isolating the relative contributions of such factors would require far more data, although the sharp decline of atmospheric carbon dioxide and methane precisely at the time of peak ice melt suggests dissolution in temporarily cold water is a major component. However, our correlations between sea ice rates, carbon dioxide rates and methane rates are the strongest with a putative driver of global greenhouse gas dynamics that we are aware of - and we

suggest they are a priority for further investigation and empirical tests of causality and mechanism. The global and Antarctic cycle of both gases have similarities suggesting the same processes or regions are involved in the dominant fluxes for both, despite their very different biological properties. Our results are consistent with stable isotopes of carbon in carbon dioxide being predominantly fractionated by sea ice formation and carbonate precipitation, rather than terrestrial photosynthesis as commonly believed; fractionation by freezing may have been underestimated (for example by Keeling et al, 2005) and should be examined in the field and with satellites giving coverage of polar regions.

If temperature drives the annual cycle of carbon dioxide and methane it should be no surprise if variation in temperature between years causes changes in the annual rate of accumulation or decline of these gases (Hambler & Henderson 2020a, b). Variation in the shape of the monthly temperature curve (*e.g.* Fig. 3c) can be used to predict variation in the monthly change of the gases - and hence monthly levels. A common mechanism could cause the observed similarity of long term changes in these gases (Salby 2012, 2013). The phase relationship between temperature and carbon dioxide has been examined to help elucidate the possible direction of causality (Granger 1969; Stips et al 2016; Faes et al 2017) and the lags we find between time series are consistent with carbon dioxide being the response variable.

The current paradigm for the carbon cycle is supported by weaker correlations than the paradigm we propose. In summary, our proposed paradigm is that the high latitude oceans are a net source of atmospheric carbon dioxide and methane due to outgassing and upwelling, punctuated annually by a brief period of oceanic drawdown when ice melts and cold water absorbs gases and impedes upwelling. Whilst paradigm shifts require strong evidence, a failure to thoroughly explore stronger correlations would be scientifically negligent. If potential processes with appropriately large magnitudes are discovered though correlations, large scale experiments will be needed to test causation. Given the high economic, social and environmental costs (Hambler & Canney 2013) of attempting to manipulate the flux of greenhouse gases it is paramount that natural fluxes be identified and partitioned to deduce the relative scale of human influence upon them.

Data availability Statement

Data are available from the sources in Table 1.

References

Bakker, D., Hoppema, M., Schröder, M. et al (2008) A rapid transition from ice covered CO_2-rich waters to a biologically mediated CO_2 sink in the eastern Weddell Gyre. *Biosciences,* **5**, 1373-1386.

Beer, C., Reichstein, M., Tomelleri, E. et al (2010) Terrestrial gross carbon dioxide uptake: global distribution and covariation with climate. *Science*, **329**, 834-838.

Brown, K.A., Miller, L.A., Mundy, C.J. et al (2015) Inorganic carbon system dynamics in landfast Arctic sea ice during the early-melt period. *Journal of Geophysical Research: Oceans*, **120**, 3542-3566.

Buermann, W., Lintner, B.R., Koven, C.D. et al (2007) The changing carbon cycle at Mauna Loa Observatory. *Proceedings of the National Academy of Sciences*, **104**, 4249-4254.

Bushinsky, S.M., Landschützer, P., Rödenbeck, C. et al (2019) Reassessing Southern Ocean air sea CO_2 flux estimates with the addition of biogeochemical float observations. *Global Biogeochemical Cycles,* **33,** 1370-1388.

Butterworth, B.J. & Miller, S.D. (2016) Air-sea exchange of carbon dioxide in the Southern Ocean and Antarctic marginal ice zone. *Geophysical Research Letters*, **43**, 7223-7230.

Ciais, P., Sabine, C., Bala, G. et al (2013) Carbon and other biogeochemical cycles. In: *Climate change 2013: the physical science basis. Contribution of Working Group I to the Fifth Assessment Report of the Intergovernmental Panel on Climate Change* (ed. by T. Stocker, D. Qin, G.-K. Plattner et al), pp. 465-570. Cambridge University Press, Cambridge, United Kingdom.

Copernicus (2019) https://atmosphere.copernicus.eu/new-high-quality-cams-maps-carbon-dioxide-surface-fluxes-obtained-satellite-observations

Damm, E., Rudels, B., Schauer, U. et al (2015) Methane excess in Arctic surface water - triggered by sea ice formation and melting. *Scientific Reports*, **5**, 16179.

Dlugokencky, E. J., Steele, L., Lang, P. M. et al (1994) The growth-rate and distribution of atmospheric methane. *Journal of Geophysical Research: Atmospheres*, **99**, 17021-17043.

Dlugokencky, E.J., Mund, J.W., Crotwell, A.M. et al (2020a) Atmospheric carbon dioxide dry air mole fractions from the NOAA GML Carbon Cycle Cooperative Global Air Sampling Network, 1968-2019, Version:

2020-07. https://doi.org/10.15138/wkgj-f215. Accessed 1 August 2020.

Dlugokencky, E.J., Crotwell, A.M., Mund, J.W. et al (2020b) Atmospheric methane dry air mole fractions from the NOAA GML Carbon Cycle Cooperative Global Air Sampling Network, 1983-2019, Version: 2020-07, https://doi.org/10.15138/VNCZ-M766. Accessed 1 August 2020.

Dlugokencky, E. (2021) Ed Dlugokencky, NOAA/GML (www.esrl.noaa.gov/gmd/ccgg/trends_ch4/). Accessed 1 January 2021.

Faes, L., Nollo, G., Stramaglia, S. et al (2017) Multiscale Granger causality. *Physical Review E*, **96**, 042150.

Fransson, A., Chierici, M., Yager, P.L. et al (2011) Antarctic sea ice carbon dioxide system and controls. *Journal of Geophysical Research: Oceans*, **116**, C12035.

Fransson, A., Chierici, M., Skjelvan, I. et al (2017) Effects of sea-ice and biogeochemical processes and storms on under-ice water fCO_2 during the winter-spring transition in the high Arctic Ocean: Implications for sea-air CO_2 fluxes. *Journal of Geophysical Research: Oceans*, **122**, 5566-5587.

Fung, I., John, J., Lerner, J. et al (1991) Three-dimensional model synthesis of the global methane cycle. *Journal of Geophysical Research*, **96**, 13033-13065.

Gagne-Maynard, W.C., Ward, N.D., Keil, R.G. et al (2017) *Frontiers in Marine Science*. 07 February 2017. https://doi.org/10.3389/fmars.2017.00026

Geilfus, N.X., Carnat, G., Dieckmann, G.S. et al (2013) First estimates of the contribution of $CaCO_3$ precipitation to the release of CO2 to the atmosphere during young sea ice growth. *Journal of Geophysical Research: Oceans*, **118**, 244-255.

Geilfus, N.-X., Tison, J.-L., Ackley, S. et al (2014) Sea ice pCO_2 dynamics and air–ice CO_2 fluxes during the Sea Ice Mass Balance in the Antarctic (SIMBA) experiment–Bellingshausen Sea, Antarctica. *Cryosphere*, **8**, 2395-2407.

Geilfus, N.-X., Galley, R., Crabeck, O. et al (2015) Inorganic carbon dynamics of melt-pond-covered first-year sea ice in the Canadian Arctic. *Biogeosciences*, **12**, 2047-2061.

Geilfus, N.-X., Pind, M., Else, B. et al (2018) Spatial and temporal variability of seawater pCO_2 within the Canadian Arctic Archipelago and Baffin Bay during the summer and autumn 2011. *Continental Shelf Research,* **156**, 1-10.

Granger, C.W.J. (1969). Investigating causal relations by econometric models and cross-spectral methods. *Econometrica,* **37**, 424-438.

Gray, A.R., Johnson, K.S., Bushinsky, S.M. et al (2018) Autonomous biogeochemical floats detect significant carbon dioxide outgassing in the high latitude Southern Ocean. *Geophysical Research Letters*, **45**, 9049-9057.

Green, J. K., Berry, J, Ciais, P., Zhang, Y. & Gentine, P. (2020) Amazon rainforest photosynthesis increases in response to atmospheric dryness. Science Advances **6**, No 47. https://www.science.org/doi/10.1126/sciadv.abb7232

Hambler, C. & Canney, S.M. (2013) *Conservation*. Cambridge University Press, Cambridge, United Kingdom.

Hambler, C. & Henderson, P.A. (2020a) Sea ice and carbon dioxide. Working Paper, version 2. https://ora.ox.ac.uk/objects/uuid:640a0c7e-6b55-4aff-a9cc-f47f6b490254

Hambler, C. & Henderson, P.A. (2020b) Sea ice and methane. Working paper, version 2. https://ora.ox.ac.uk/objects/uuid:52b0e80f-7358-4b88-8941-55068738638e.

Harris, N.L., Gibbs, D.A., Baccini, A. et al (2021) Global maps of twenty-first century forest carbon fluxes. *Nature Climate Change*, **11**, 234–240

He, Z.H., Zeng, Z.C., Lei, L.P. et al (2017) A data-driven assessment of biosphere-atmosphere interaction impact on seasonal cycle patterns of XCO_2 Using GOSAT and MODIS observations. *Remote Sensing*, 2017, **9**, 251.

Heimann, M., Keeling, C.D. & Tucker, C.J. (1989) A three-dimensional model of atmospheric CO_2 transport based on observed winds: 3. Seasonal cycle and synoptic time scale variations. *Aspects of climate variability in the Pacific and the Western Americas, Geophysical Monograph,* **55**, 277-303.

Hein, R., Crutzen, P. J. & Heimann, M. (1997) An inverse modelling approach to investigate the global atmospheric methane cycle. *Global Biogeochemical Cycles*, **11**, 43-76.

Henderson, P.A. (2021) *Southwood's Ecological Methods*. 5th Edn. Oxford University Press, Oxford, United Kingdom.

Humlum, O., Stordahl, K. & Solheim, J.-E. (2013) The phase relation between atmospheric carbon dioxide and global temperature. *Global and Planetary Change,* **100,** 51-69.

IPCC (2013) *Climate Change 2013: The physical science basis. Contribution of Working Group I to the Fifth Assessment Report of the Intergovernmental Panel on Climate Change* (ed. by T. Stocker, D. Qin, G.-K. Plattner et al), Cambridge University Press, Cambridge, United Kingdom.

Ishii, M., Inoue, H.Y. & Matsueda, H. (2002) Net community production in the marginal ice zone and its importance for the variability of the oceanic pCO2 in the Southern Ocean south of Australia. *Deep Sea Research Part II: Topical Studies in Oceanography*, **49**, 1691-1706.

Jackowicz-Korczyński, M., Christensen, T.R., Bäckstrand, K. et al (2010) Annual cycle of methane emission from a subarctic peatland. *Journal of Geophysical Research*, **115**, G02009.

Jiang, X. & Yung, Y.L. (2019) Global patterns of carbon dioxide variability from satellite observations. *Annual Review of Earth and Planetary Sciences,* **47**, 225-245.

Keeling, C.D., Bacastow, R.B., Carter, A. et al (1989) A three-dimensional model of atmospheric CO_2 transport based on observed winds: 4. Mean annual gradients and interannual variations. *Aspects of climate variability in the Pacific and the Western Americas, Geophysical Monograph,* **55,** 305-363.

Keeling, C.D., Piper, S.C., Bacastow, R.B. et al (2005). Atmospheric CO_2 and $^{13}CO_2$ exchange with the terrestrial biosphere and oceans from 1978 to2000: observations and carbon cycle implications. In EPRINTS-BOOK-TITLE University of Groningen, Centre for Isotope Research.

Keeling, C.D., Piper, S.C, Bacastow, R.B. et al (2001) Exchanges of atmospheric CO_2 and $^{13}CO_2$ with the terrestrial biosphere and oceans from 1978 to 2000. In: *Exchanges of atmospheric* CO_2 *and* $^{13}CO_2$ *with the terrestrial biosphere and oceans from 1978 to 2000. I. Global aspects, SIO Reference Series, No. 01-06*, pp. 1-88. Scripps Institution of Oceanography, San Diego.

Keeling, R.F. (2008) Recording Earth's vital signs. *Science,* **319,** 1771-1772.

Kort, E. A., Wofsy, S. C., Daube, B. C. et al (2012) Atmospheric observations of Arctic Ocean methane emissions up to 82 degrees north. *Nature Geoscience*, **5**, 318-321.

Mastepanov, M., Sigsgaard, C., Dlugokencky, E.J. et al (2008) Large tundra methane burst during onset of freezing. *Nature*, **456,** 628–630.

Mearns, E. (2015). CO2 - The view from space - update. http://euanmearns.com/co2-the-view-from-space-update/ Accessed 24 April 2021.

MOSAiC (2019) The key to the Arctic puzzle. From https://www.mosaic-expedition.org/science/arctic-climate/. Accessed 29 October 2019.

Nelson, M.D. & Nelson, D.B. (2016) Oceans, ice & snow and CO_2 rise, swing and seasonal fluctuation. *International Journal of Geosciences*, **7**, 1232-1282.

Niles, P.B., Socki, R.A. & Hredzak, P.L. (2007) A new method for evaluating the carbon isotope characteristics of carbonate formed under cryogenic conditions analogous to Mars. *Lunar and Planetary Science,* **XXXVIII**.

Nomura, D., Eicken, H., Gradinger, R. et al (2010) Rapid physically driven inversion of the air–sea ice CO_2 flux in the seasonal landfast ice off Barrow, Alaska after onset of surface melt. *Continental Shelf Research*, **30**, 1998-2004.

Nomura, D., Granskog, M.A., Assmy, P. et al (2013) Arctic and Antarctic sea ice acts as a sink for atmospheric CO_2 during periods of snowmelt and surface flooding. *Journal of Geophysical Research: Oceans*, **118**, 6511-6524.

Nomura, D., Yoshikawa-Inoue, H., Kobayashi, S. et al (2014) Winter-to-summer evolution of pCO_2 in surface water and air–sea CO_2 flux in the seasonal ice zone of the Southern Ocean. *Biogeosciences*, **11**, 5749-5761.

Nomura, D., Granskog, M.A., Fransson, A. et al (2018) CO_2 flux over young and snow-covered Arctic pack ice in winter and spring. *Biogeosciences,* **15**, 3331-3343.

Ouyang, Z., Qi, D., Chen, L. et al. (2020) Sea-ice loss amplifies summertime decadal CO_2 increase in the western Arctic Ocean, *Nature Climate Change*. https://doi.org/10.1038/s41558-020-0784-2 Accessed 18 June 2020.

Park, J. (2009) A re-evaluation of the coherence between global-average atmospheric CO_2 and temperatures at interannual time scales. *Geophysical Research Letters*, **36**, L22704.

Prytherch, J., Brooks, I.M., Crill, P.M. et al (2017) Direct determination of the air-sea CO_2 gas transfer velocity in Arctic sea ice regions. *Geophysical Research Letters*, **44**, 3770-3778.

Qin, Y, Xiao, X., Wigneron, J.-P. et al (2021) Carbon loss from forest degradation exceeds that from deforestation in the Brazilian Amazon. *Nature Climate Change* **11**, 442-48.

Ravishankara, A.R. & Albritton, D.L. (1995) Methyl chloroform and the atmosphere. *Science*, **269**, 183-184.

Reidel, K. & Lassey, K. (2008) "Detergent of the atmosphere". *Water & Atmosphere*, **16**, 22-23.

Rentsch, C. (2021a) https://twitter.com/crentsch/status/1358122750259441666

Rentsch, C. (2021b) Radiative forcing by CO_2 observed at top of atmosphere from 2002-2019. https://arxiv.org/abs/1911.10605

Resplandy, L., Keeling, R., Rödenbeck, C. et al (2018) Revision of global carbon fluxes based on a reassessment of oceanic and riverine carbon transport. *Nature Geoscience,* **11,** 504-509.

Roden, N.P., Tilbrook, B., Trull, T.W. et al (2016) Carbon cycling dynamics in the seasonal sea ice zone of East Antarctica. *Journal of Geophysical Research: Oceans*, **121**, 8749-8769.

Salby, M. (2012) *Physics of the atmosphere and climate*, 2nd edn. Cambridge University Press, Cambridge, United Kingdom.

Salby, M. (2013) Presentation Prof. Murry Salby in Hamburg on 18 April 2013. https://www.youtube.com/watch?v=2ROw_cDKwc0&feature=youtu.be. Accessed 9 February 2021.

Saunois, M., Stavert, A. R., Poulter, B. et al (2020) The Global Methane Budget 2000-2017. *Earth System Science Data*, **12**, 1561-1623.

Sejr, M.K., Krause-Jensen, D., Rysgaard, S. et al (2011) Air-sea flux of CO_2 in Arctic coastal waters influenced by glacial melt water and sea ice. Tellus B: *Chemical and Physical Meteorology*, **63**, 815-822.

Semiletov, I.P., Pipko, I.I., Repina, I. et al (2007) Carbonate chemistry dynamics and carbon dioxide fluxes across the atmosphere–ice–water interfaces in the Arctic Ocean: Pacific sector of the Arctic. *Journal of Marine Systems*, **66**, 204-226.

Shadwick, E.H., Thomas, H., Chierici, M. et al (2011) Seasonal variability of the inorganic carbon system in the

Amundsen Gulf region of the southeastern Beaufort Sea. *Limnology and Oceanography*, **56**, 303-322.

Sitch, S., Friedlingstein, P., Gruber, N. et al (2015) Recent trends and drivers of regional sources and sinks of carbon dioxide. *Biogeosciences*, **12**, 653-679.

Søgaard, D.H., Deming, J.W., Meire, L. et al (2019) Effects of microbial processes and $CaCO_3$ dynamics on inorganic carbon cycling in snow-covered Arctic winter sea ice. *Marine Ecology Progress Series*, **611**, 31-44.

Stips, A., Macias, D., Coughlan, C. et al (2016) On the causal structure between CO_2 and global temperature. *Scientific Reports*, **6**, 1-9.

Tison, J.-L., Delille, B. & Papadimitriou, S. (2017) Gases in sea ice. In: *Sea ice*, 3rd edn. (ed. by D.N. Thomas), pp. 433-471. Wiley, New Jersey.

UNESCO, WRI, IUCN (2021) *World Heritage forests: Carbon sinks under pressure.* UNESCO, Paris.

Vancoppenolle, M., Meiners, K.M., Michel, C. et al (2013) Role of sea ice in global biogeochemical cycles: emerging views and challenges. *Quaternary Science Reviews*, **79**, 207-230.

Vancoppenolle, M. & Tedesco, L. (2017) Numerical models of sea ice biogeochemistry. In: *Sea ice*, 3rd edn. (ed. by D.N. Thomas), pp. 492-515. Wiley, New Jersey.

Weber, T., Wiseman, N. A. & Kock, A. (2019) Global ocean methane emissions dominated by shallow coastal waters. *Nature Communications*, **10**, 4584.

Welp, L.R., Patra, P.K., Rödenbeck, C. et al (2016) Increasing summer net CO2 uptake in high northern ecosystems inferred from atmospheric inversions and comparisons to remote-sensing NDVI. *Atmospheric Chemistry and Physics*, **16**, 9047-9066.

White, J.W.C., B.H. Vaughn, and S.E. Michel (2015), University of Colorado, Institute of Arctic and Alpine Research (INSTAAR), Stable Isotopic Composition of Atmospheric Carbon Dioxide (13C and 18O) from the NOAA ESRL Carbon Cycle Cooperative Global Air Sampling Network, 1990-2014, Version: 2015-10-26, Path: ftp://aftp.cmdl.noaa.gov/data/trace_gases/co2c13/flask/

Wiesenburg, D.A. & Guinasso Jr, N.L. (1979) Equilibrium solubilities of methane, carbon monoxide, and hydrogen in water and sea water. *Journal of Chemical and Engineering Data,* **24,** 356-360.

Winkler, A.J., Myneni, R.B., Alexandrov, G.A. et al (2019) Earth system models underestimate carbon fixation by plants in the high latitudes. *Nature Communications,* **10,** 1-8.

Zhao, F., Zeng, N., Asrar, G. et al (2016) Role of CO_2, climate and land use in regulating the seasonal amplitude increase of carbon fluxes in terrestrial ecosystems: a multimodel analysis. *Biogeosciences*, **13**, 5121–5137.

Acknowledgements

Download and processing of MODIS satellite imagery was implemented by Environmental Research Group Oxford, Ltd. and we thank William Wint for this and for critical comment. Several colleagues and particularly Marian Dawkins provided valuable critiques. We thank all sources listed in Table 1 or indicated in the metadata on the hosting websites: the effort of collecting and curating valuable long-term data is enormous.

Author Contributions

CH and PAH contributed equally.

Declarations

Funding None.

Conflict of interest / Competing Interest Statement The authors have no conflict of interest / competing interests.

Data Availability Statement Data are available from the online providers indicated in Table 1. R code can be provided upon reasonable request.